2022-07

Effects of navier slip and skin friction on nanofluid flow in a porous pipe

Muyungi, Wivina

NM-AIST

EFFECTS OF NAVIER SLIP AND SKIN FRICTION ON NANOFLUID FLOW IN A POROUS PIPE

Wivina Nathan Muyungi

A Dissertation Submitted in Partial Fulfilment of the Requirements for the Degree of Master's in Mathematical and Computer Sciences and Engineering of the Nelson Mandela African Institution of Science and Technology

Arusha, Tanzania

July, 2022

ABSTRACT

Recent advances in cooling, filtering, heat transfer, and other processes have all focused attention on fluid flow through porous media. During the flow partial slip becomes more important at wall surfaces in improvement of performance of various devices. In this regard, the governing equation has been presented for the flow of porous pipe with Navier slip in this study also non dimensionalisation has been done. Systems of equations The governing system was expressed to ordinary differential equations, thereafter a mathematical model for the flow of nanofluids was developed. Results are presented graphically of various parameters having different values on and discussed. It is found that the velocity and temperature during the flow is inversely proportional to Navier slip also in order to overcome skin friction there is a need to increase nanoparticles.

DECLARATION

I, Wivina Nathan Muyungi do hereby declare to the Senate of the Nelson Mandela African Institution of Science and Technology (NM-AIST) that this dissertation is my original work and that it has neither been submitted nor being presented for any degree award in any other Institution.

Wivina Nathan Muyungi   19th July, 2022
Name of the Candidate   **Signature**   **Date**

The above declaration is confirmed

Prof. Verdiana Grace Masanja   19th July, 2022
Supervisor 1   **Signature**   **Date**

Dr. Michael Hamza Mkwizu   19th July, 2022
Supervisor 2   **Signature**   **Date**

COPYRIGHT

CERTIFICATION

The undersigned certify that they have read and hereby recommend for examination of a dissertation entitled: Effects of navier slip and skin friction on nanofluid flow in a porous pipe, in partial fulfillment of the requirements for the Master Degree in Applied Mathematics of the Nelson Mandela African Institution of Science and Technology (NM-AIST) Arusha, Tanzania.

Prof. Verdiana Grace Masanja   19th July, 2022
Supervisor 1   **Signature**   **Date**

Dr. Michael Hamza Mkwizu   19th July, 2022
Supervisor 2   **Signature**   **Date**

ACKNOWLEDGEMENT

DEDICATION

I dedicate this work to all my family members.

TABLE OF CONTENTS

LIST OF TABLES

LIST OF FIGURES

LIST OF ABBREVIATIONS AND SYMBOLS

ρ_{nf}	Nanofluid Density
μ	Dynamic Viscosity
μ_k	Kinematic Viscosity
k_{nf}	Nanofluid thermal conductivity
τ	Ratio of Solid Particles Heat Capacitance to That of the Nanofluid Heat Capacitance
φ	Concentration of Nanoparticles,
c_p	Specific Heat Capacity at Constant Pressure
u_r, u_θ, u_z	Fluid Velocity Components Along the r, θ and z Directions Respectively
(r, θ, z)	Cylindrical Coordinates
β	Navier Slip Parameter
T	Nanofluid Temperature
T_a	Ambient Temperature
Bi	Local Biot Number
Pr	Prandtl Number
Ec	Eckert Number
A	Pressure Gradient Parameter
C_f	Skin friction Coefficient
Nu	Local Nusselt Number
ϑ	Nanoparticles Volume Fraction
ρ	Density of the Fluid
α_f	Thermal Diffusivity Of The Fluid
ρ_s	Density of the Nanoparticles
$(\rho c_p)_f$	Heat Capacitance of the Base Fluid
$(\rho c_p)_{nf}$	Heat Capacitance of the Nanoparticle
τ_w	Wall shear Stress
P	Pressure

CHAPTER ONE

INTRODUCTION

1.1 Background of the problem

Fluid flow through porous media takes place in a number of technical areas including ground water flows, flow through embankment dams, waste water treatment and filtering. The flow of fluid in porous conduits or pipes is governed by pressure differential between inlet and outlet of the pipelines and flow of fluid flow in channels or canals is influenced by gravity. But a flow of the fluid through a porous medium under Navier slip condition that is derived as the effective boundary condition, in the limit as the roughness becomes small; is the first order corrector to the no-slip boundary condition on the limiting smooth surface.

There are three possibilities as the fluid substance comes into contact with the flow medium's wall surface. Three scenarios are depicted in Fig. 1.
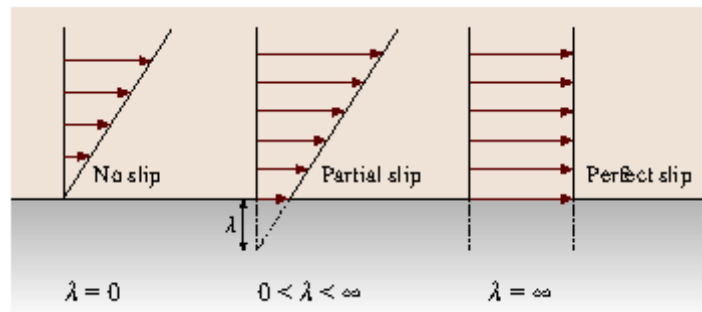
Figure 1: Interpretation of three option of slip flow

Which are (a) no slip (stagnant, this indicates that the substance adheres to the surface), (b) partial slip (indicates the penetration of fluid to a lesser or greater degree past the wall), and (c) complete slip (the coefficient of viscosity equals to a unity, meaning no friction force whatsoever) (Fang et $al.$, 2010; Muravleva, 2017; Sochi, 2011). Most studies consider a no-slip wall boundary condition. Since there are several studies which has been done in slip and the results shows that has wall slip bought different significance at the wall (Eijkel, 2007). This condition was first introduced by Navier in 1827 (Wang & Ng, 2011). His model describes that boundary slip velocity (U_s) is proportional to shear rate ($\dot{\gamma}$) slip length (λ) which is proportionality constant remains constant (Fig. 2).

1
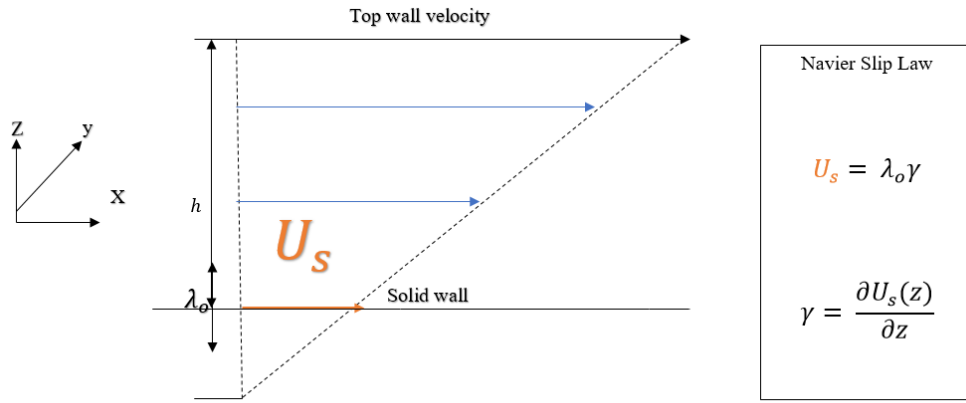
Figure 2: Enrichment of flow velocity U$_s$ as a result of the boundary slip conditions

Mathematically, this can be expressed as;

$$U_s = \lambda \dot{\gamma} \, , \tag{1.1}$$

Where $\dot{\gamma} =$

$$\frac{dU_x(z)}{dz} \quad . \tag{1.2}$$

Actually, some studies Hussain *et al*. (2016); Nair and Sameen, 2015; Sochi, 2011) have shown that several different materials, including polymers and nanofluids, has a slip on a solid surfaces. Mathematical studies of fluid flow of such materials generate flow patterns which help the manufacturers to design, manufacturing processes as the flow pattern has a major impact based on the properties of the final product material. Precise and accurate prediction of the mathematically produced flow patterns is important in determining the fibre orientation as well as the hardening behaviour of the treated material in the compression molding of fiber-reinforced composites (Hussain *et al*., 2016). Also, studies have established that overall stress levels are lowered by the controlled level of partial slip. Also it id found that in future partial slip will be more considered since it simplifies the design and various devices used in industry and engineering work for instance, fluid transportation and material processing, (Kalyon, 2005).

Skin friction is a drag that develops when a fluid rubs up against the surface of a moving object. And thus has impacts on the amount of energy used. When the drag is decreased, an object or fluid moving forward through a specific medium performs better. Flack *et al*. (2016) investigated on how roughness can cause skin friction inside the pipe during the movement of

fluid inside a pipe. The results observed is that in order to overcome skin friction the measurement of roughness should be identified.

Recently, nanofluid flow in porous media has received considerable attention in many fundamental heat transfer analyses due to their wide range of applications in high performance insulation, for example, grain storage, buildings, packed sphere beds, chemical catalytic reactors and geophysical issues such as frost surge (Erdoğan & Imrak, 2008; Khamis, 2016).

In this study, there is a gap appeared in the literature, so a mathematical model is developed and utilized to investigate the impact of Navier slip and skin friction of nanofluid flow in a porous conduit.

1.1.1 Nanofluid

Choi (1995) originally proposed the concept of nanofluid (Fig. 3), which is a fluid with some types of Nano-metric particles suspended in a base fluid like water, engine oil, and ethylene glycol (Rawi *et al*., 2017). Examples of nanoparticles are carbide ceramics (SiC, TiC), nitride ceramics (AlN, SiN), alloyed nanoparticles (Al70, Cu30), metals (Cu, Ag, Au), semiconductors (TiO2, SiC), single, double or multi walled carbon nanotubes, metallic oxides (Al2O3, CuO), etc.

There are properties which play important role in the preparation of nanofluids through they respond differently when is added to the fluid. Those properties are viscosity, specific heat, thermal Conductivity and Stability because every nanoparticle. Compared to pure liquid and regular solid–liquid suspension, nanofluids offer the following advantages: higher specific surface area, which increases heat transfer between particles and surface fluids, high thermal conductivity and has high thermal transfer.
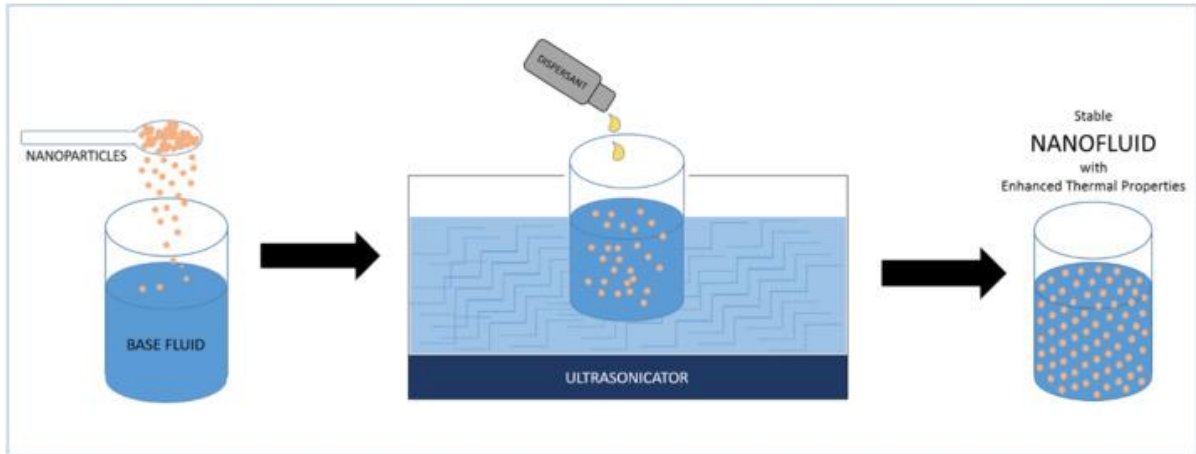
Figure 3: Nanofluid

1.1.2   Porous pipe

Porous pipe is the pipe channel permeable walls (Fig. 4). The walls are interconnected in such a way that fluid can flow through the media. Porous media have several industrial applications, including: petroleum engineering, chemical engineering, Hydrogeology (for instance during floods or storm-water, porous or perforated pipes are installed below the ground to perform drainage of flooded water), civil engineering (in a bridge and culvert constructions as well as porous or permeable concrete), medicine and Pharmaceutical company (biomedical engineering), The treatment of drinking water and the treatment of beverages and filtration processes entail a tangential flow of the fluid over a porous wall. In general, the flow is driven by a pressure differential (the potential gradient between two points accounts for the fluids movement from the point with high potential towards the lower potentiometric pressure point). When a fluid is flowing in pipe skin friction (friction loss) occurs in the pipe wall or conduit due to the effect of fluid viscosity near the pipe surface or conduit.
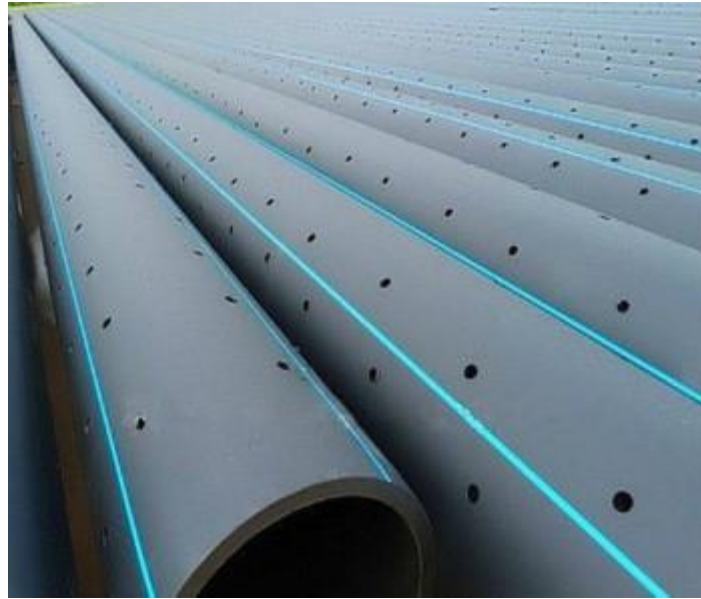
Figure 4: Porous HDPE pipe for Drainage

1.2 Statement of problem

The study of Navier slip of nanofluid flow in a different media has been investigated by various researchers as explained in Section 1.1. The researchers have considered the combined effect of various parameters such as buoyancy-driven force, variable viscosity, magnetic flied and others in different cases such as on heat transfer and in the unsteady and steady flow situations in various media. There is a need to do more study of Navier slip on a porous pipe since the flow in fluid in porous pipe continues to be a big problem, whose effect results in lowering the performance of thermodynamic systems. Generally, it affects the efficiency of the system. Therefore, the mathematical models will be developed and used to analyse the flow of nanofluids in a porous pipe in this study since there is a need of more investigation to be done in this area.

1.3 Rationale of the study

Various studies on porous pipe have been conducted in order to overcome the different problems. This study is not yet being done and is focusing on modelling the Navier slip condition of nanofluid flow in a porous pipe. The identified effect will provide useful information to engineers in designing smallest heat exchanger systems which works with high efficiency and low cost.

1.4   Research objectives

1.4.1   The general objective

The general objective of this research is to develop a mathematical model of nanofluid flow in a porous pipe and use the model to analyse the effect of Navier slip condition on skin friction.

1.4.2   Specific objectives

(i)   To formulate flow model for a case of nanofluid in a porous pipe.

(ii)   To determine the effect of various parameters on the velocity and temperature profiles.

(iii) To analyze the results of Reynold's number, Eckert number, Nusselt number, Prandtl number, pressure gradient, concentration of volume fraction of parameter and Navier slip on the skin friction and Nusselt number.

1.5   Research questions

(i)   Which models of nanofluid flow in a porous pipe can be formulated?

(ii)   What is the impact of different parameters on velocity profile and temperature profiles in nanofluid flow?

(iii) What is the impact of various parameters and Navier slip on the skin friction and Nusselt number?

1.6   Significance of the research

(i)   To assist engineers and other interested people with more/new knowledge to the existing one on modelling skin friction and Navier slip of nanofluid flow in porous pipe.

(ii)   It helps the engineers to decide on the best control measures of eddy loss of fluid due to friction porous pipe,

(iii) The study provides insight into solutions to maintain the temperature of the transferring fluid and linkage of porous pipe.

(iv)   Opportunity of extending the research.

1.7   Delineation of the study

This study is focused on the flow only in porous pipe with nanofluid moving through the pipe having copper and alumina nanoparticles. Also assumptions where implemented to come up with the model during the flow.

2.1   Introduction

This chapter focuses on a literature review of nanofluid flow. The review of this work is categorized into two categories which are nanofluid flow in porous pipe and the effect of different parameters of nanofluid flow in various mediums with Navier slip.

2.2   Nanofluid flow in Porous Pipe

Mari *et al*. (1987) studied the modelling of the skin friction and heat transfer in turbulent two-component bubbly flows in pipe, the results observed from the generated model is that the rise of heat-transfer and skin friction is due to the increase of velocity of two phases and values of the Prandtl number.

Erdoğan and Imrak (2008) studied on uniformly porous pipe considering the flow of fluid with suction and injection. The results found are the pressure for flow in a more porous pipe than the pressure for flow in a non-porous pipe. Also, similarities between flow in a uniform porous pipe and flow in a rectangular porous pipe with suction and injection was observed.

Srinivas *et al*., (2015) studied on chemical reaction and mass transfer impact on laminar flow in a porous pipe with an contracting or expanding wall. The rate of wall expansion was found greatly increases the axial speed and lowers the axial speed in the case of wall contraction, whatever the injection or suction. Concentration decreases with the increasing Schmidt numbers.

Mahmoudi and Karimi (2014) studied on the heat transfer by forced convection in a pipe partially filled with a porous material result showed that the Darcy number and thickness are inversely proportional.

Nouri-Borujerdi (2015) studied on forced convection the flow considered was turbulent and heat in a porous pipe result found are as the thickness of the porous medium increases, the local Nusselt number along the pipe approaches a constant value. In addition, when the Darcy number decreases, the fluid velocity inside the porous medium decreases, while the velocity

outside the porous region increases at the expense of a reasonable pressure drop, which depends on the permeability of the porous matrix.

Srinivas *et al*. (2016) studied in the presence of a heat source/sink, the results of chemical reaction on MHD flow of a nanofluid through a porous pipe that is contracting or expanding. It was found that the heat source raises the temperature while the heat sink lowers it in all the cases of wall contraction and expansion coupled with an injection. In addition, the temperature increased substantially with a rise in the value of Brownian motion and thermophoresis parameters.

Barik *et al*. (2017) investigated on the influence of porous matrix, elasticity, injection/suction and viscous-elastic fluid inlet flow through a porous pipe. It was observed that elasticity and suction work against increased skin friction, making them useful for managing flow separation. Also the presence of a porous matrix and a magnetic field lead to a slightly asymmetric flow relative to the pipe's core.

Kasaeian *et al*. (2017) investigated the usage of porous media and heat transfer nanofluids. He found that using porous media and nanofluids improves the heat transfer rate in the system. Moreover, nanofluid ameliorate the performance.

Gadanga *et al*., (2020) investigated the heat absorption on free convection flow past a vertical porous pipe with mass transfer. It is observed that the velocity becomes higher when thermal Grashof number and suspension parameter are increased. Also, increase in magnetic parameter, Schmidt and Prandtl numbers lead to fall in the velocity of the fluid. The fluid temperature rises also due to the increase in heat generation, but reduces for increased value of Prandtl number. Therefore, by raising the Schmidt values, the concentration limit layer decreases.

2.3   Nanofluid Flow with Navier slip

Many fields of industry, science and engineering are affected by the wall slip. Since many activities in engineering occur at high temperature has become so essential in the design of dependable equipment, such as gas turbines, nuclear power plants and various propulsion systems for aircraft, rockets, satellites, and space vehicles (Hussain *et al*., 2016). On the basis of these applications different studies have been conducted with Navier slip in consideration.

Eegunjobi and Makinde (2012) studied combined suction/injection and asymmetric Navier slip outcomes in a porous channel happened because of the production of entropy in the flow. They found that the transfer of heat irreversibility controls the flow process in the channel.

Mutuku *et al*. (2013) examined on the influence of a magnetic field on the boundary layer flow of nanofluids past a vertical porous convectively heated plate with the Navier slip boundary condition the findings show that fluid velocity increase but due to the rise in slip parameters there is a decrease in skin friction. Thermal border layer thickness and temperature are elevated.

Makinde *et al*. (2014) studied on heat transfer in Berman flow of nanofluid with Navier Slip. The results reveal that the Biot number is inversely proportional to temperature also both temperature, velocity and heat transfer coefficient (Nu) are directly proportional to the Reynolds number and Navier slip.

Rundora and Makinde (2014) investigated the effect of suction/injection, Navier slip, convective cooling and temperature dependent viscosity of fluid flowing unsteadily in a porous channel. They found that the suction/injection Reynolds number delays fields of temperature and velocity as well as skin friction increases due to the number of Prandtl, the number of Reynolds and the slip parameter. The different effects occurred because of the porous medium shape and variable viscosity parameters.

Khamis *et al*. (2015) studied on the results of buoyancy-driven force, temperature dependent viscosity and Navier slip on transfer of heat in a permeable cylindrical pipe it was found that all nanofluid velocity and temperature are intensified by Grashof number and adding nanoparticles volume fraction and minimized by increasing Navier slip parameter, viscosity , resistance and shape factor parameters of porous media.

Mkwizu *et al*. (2015) investigated on heat transfer in permeable walls with Navier slip on entropy generation in Couette flow between two parallel plates. They found that skin friction and temperature is directly proportional to slip parameter, nanoparticles volume fraction and Reynolds number. But inversely proportional to pressure gradient.

Hussain *et al*. (2016) showed the results of variable viscosity, partial slip, and variable thermal conductivity on steady boundary layer nanofluid flow over a porous sheet and found that due to the increase in viscosity of nanofluid, velocity and porous medium permeability cause the

decrease of, thermal boundary layer thickness, momentum and slip parameter which in the end increased the rate of transferring of heat.

Flack *et al*. (2016) investigated on how roughness can cause skin friction inside the pipe during the movement of fluid inside a pipe. The results observed is that in order to overcome skin friction the measurement of roughness should be identified.

Pandey and Kumar (2017) studied the heat flow with slip in a porous cylinder. It has been found that slip and radiation parameters varies inversely proportional to Nusselt number but directly proportional to velocity. Skin friction decreases as the numerical values of heat generation /absorption and thermal radiation increase.

Bhatti *et al*. (2018) discussed the Newtonian fluid passing a cylindrical pipe flowing unsteadily with slip at the wall. It has been found that the magnitude of axial velocity component increases with the increase in the numerical value of partial slip.

In this study, a mathematical model is developed to study the effect of various parameter on the velocity and temperature profiles, also skin friction and Nusselt number of nanofluid flow in porous pipe because is not yet being done in previous research.

CHAPTER THREE

MATERIALS AND METHODS

3.1 Introduction

This section describes methods, materials and techniques that have been used to develop the nanofluid flow model in a porous pipe. In addition, other concepts are presented that are of paramount importance in developing the model.

3.2 Governing equation

Fluid flow is described by fundamental equations which reflects the well-known laws of mechanics namely; continuity, momentum and energy equations. The mass conservation principle underpins the continuity equation, newton's second law of motion is used to derive the momentum equation and the law of conservation of energy is used to derive the energy equation. The equations can be expressed in different forms like cartesian coordinate, polar coordinate and so on. The general form of the governing equations is provided and well explained in this Section.

3.2.1 The continuity equation

In this section of nanofluid flow, the principle of mass conservation will be used. For a fixed finite control volume in space the law of conservation of mass states that "The net rate at which mass enters the control volume equals the rate at which the mass of the material increases within the control volume" (Fig. 5).
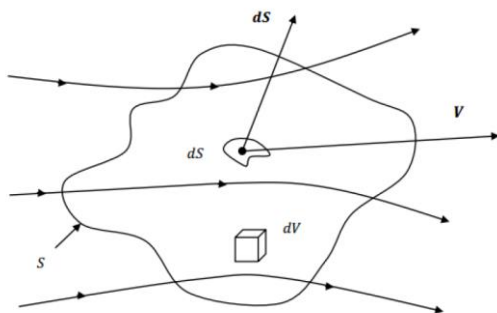
Figure 5: Finite control volume fixed space

We have a closed surface (S) which bounds the volume. The control volume (V) may be fixed in space with the fluid moving through It. Consider the relation that the total mass M in the control volume V is obtained by integrating the product of differential volume and density (ρ).Thus;

$$M = \int \rho \, dV, \tag{3.1}$$

The rate of mass of the material increases is given by:

$$\frac{dM}{dt} = \int \frac{d\rho}{dt} dV, \tag{3.2}$$

Net rate of entry of mass into the control volume through the control surface (S) is obtained by integrating the product of density, velocity vector (V) and differential area (dS).

$$-\frac{dM}{dt} = \int \rho \, \vec{V} dS, \tag{3.3}$$

Where the sign minus means the rate mass decreases

Equation (3.2) must be equal to equation (3.3) according to the principle of mass conservation: Thus;

$$\int \rho \, V dS = -\int \frac{d\rho}{dt} dV, \tag{3.4}$$

$$\int \frac{d\rho}{dt} dV + \int \rho \, V dS = 0, \tag{3.5}$$

Using the Gauss divergence theorem, the surface integral in equation (3.5) can be written as a volume integral,

$$\int \rho V dS = \int \nabla \cdot (\rho V) \, dV, \tag{3.6}$$

Substituting equation (3.6) into equation (3.5) we will have:

$$\int \left[\frac{d\rho}{dt} + \nabla \cdot (\rho V) \right] dV = 0, \tag{3.7}$$

The integrand must be zero for the integral in the equation (3.8) to be met because the finite control volume is drawn randomly in space and position. Therefore:

$$\frac{d\rho}{dt} + \nabla.(\rho V) = 0. \tag{3.8}$$

where,

$$\nabla \equiv \frac{\partial}{\partial u} + \frac{\partial}{\partial v} + \frac{\partial}{\partial w}$$

Equation (3.5) is continuity equation in differential form.

In Cartesian coordinate with $V = (u, v, w)$ we will have:

$$\frac{\partial\rho}{\partial t} + \left[\frac{\partial(\rho u)}{\partial x} + v\frac{\partial(\rho v)}{\partial y} + \frac{\partial(\rho w)}{\partial z}\right] = 0. \tag{3.9}$$

In cylindrical polar coordinates (r, θ, z) with $V = (u_r, u_\theta, u_z)$, and that the continuity equations, in 3D is given by equation (3.5):

$$\frac{\partial\rho}{\partial t} + \frac{1}{r}\frac{\partial(r\rho u_r)}{\partial r} + \frac{1}{r}\frac{\partial(\rho u_\theta)}{\partial\theta} + \frac{\partial(\rho u_z)}{\partial z} = 0. \tag{3.10}$$

3.2.2 Momentum equation

In fluid motion, the momentum equation is another expression of Newton's Second Law of Motion, which states that "the rate of change of momentum of the matter is equal to the net external forces acting on it". In the derivation of flow model (Fig. 6).
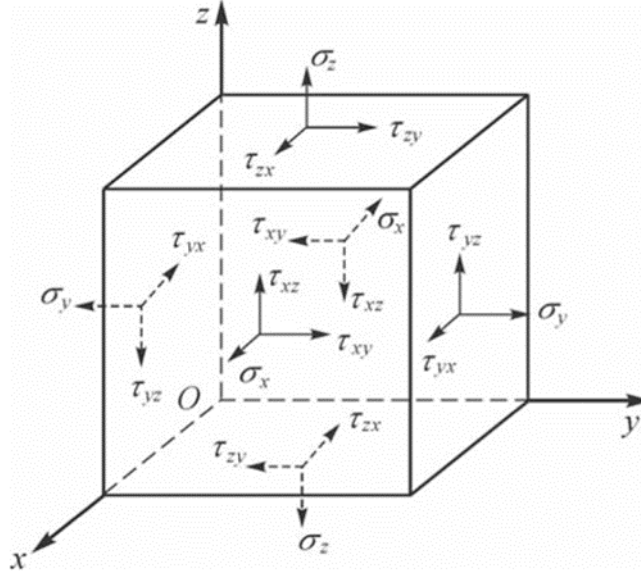
Figure 6: Infinitesimally small fluid element in motion

By applying Newton's second law to an infinitesimal element 3D substantial derivative in Cartesian coordinates is given by:

$$\frac{D}{Dt} \equiv \frac{\partial}{\partial t} + u\frac{\partial}{\partial x} + v\frac{\partial}{\partial y} + w\frac{\partial}{\partial z}. \tag{3.11}$$

Equation (3.11) can be written in terms of the operator ∇ as:

$$\frac{D}{Dt} \equiv \frac{\partial}{\partial t} + (V.\nabla). \tag{3.12}$$

Which has two parts, (i) $\frac{\partial}{\partial t}$ is the *local derivative* implies that time rate of change at a fixed point; and (ii) $V.\nabla$ the *convective derivative* which is time rate of change due to the movement of the fluid element.

Acceleration is defined by:

$$a = \frac{DV}{Dt} = \frac{\partial V}{\partial t} + V(V.\nabla), \tag{3.13}$$

From Newton's second law of motion

$$F = ma, \tag{3.14}$$

$$F = \rho\frac{DV}{Dt}dxdydz, \tag{3.15}$$

Where

F is external forces operating on the fluid element which are surface and body forces such as:

$F = F_s + F_b$

$m =$ is mass

The sum of the forces $(F = F_s + F_b)$ by considering x, y and z directions will be:

$$F_X = \left(-\frac{\partial p}{\partial x} + \frac{\partial \tau_{xx}}{\partial x} + \frac{\partial \tau_{yx}}{\partial y} + \frac{\partial \tau_{zx}}{\partial z}\right) dxdydz + \rho f_x dxdydz,$$

$$F_Y = \left(-\frac{\partial p}{\partial y} + \frac{\partial \tau_{xy}}{\partial x} + \frac{\partial \tau_{yy}}{\partial y} + \frac{\partial \tau_{zy}}{\partial z}\right) dxdydz + \rho f_y dxdydz, \qquad (3.16)$$

$$F_Z = \left(-\frac{\partial p}{\partial z} + \frac{\partial \tau_{xz}}{\partial x} + \frac{\partial \tau_{yz}}{\partial y} + \frac{\partial \tau_{zz}}{\partial z}\right) dxdydz + \rho f_z dxdydz,$$

Substitute equation (3.16) in equation (3.15) we will have:

$$\left(-\frac{\partial p}{\partial x} + \frac{\partial \tau_{xx}}{\partial x} + \frac{\partial \tau_{yx}}{\partial y} + \frac{\partial \tau_{zx}}{\partial z}\right) + \rho f_x = \rho \frac{Du}{Dt},$$

$$\left(-\frac{\partial p}{\partial y} + \frac{\partial \tau_{xy}}{\partial x} + \frac{\partial \tau_{yy}}{\partial y} + \frac{\partial \tau_{zy}}{\partial z}\right) + \rho f_y = \rho \frac{Dv}{Dt}, \qquad (3.17)$$

$$\left(-\frac{\partial p}{\partial z} + \frac{\partial \tau_{xz}}{\partial x} + \frac{\partial \tau_{yz}}{\partial y} + \frac{\partial \tau_{zz}}{\partial z}\right) + \rho f_z = \rho \frac{Dw}{Dt},$$

Equation (3.17) is momentum equation in substantial derivative definition will be written as:

$$\rho \frac{DV}{Dt} = \rho \frac{\partial u}{\partial t} + \rho V.\nabla u, \qquad (3.18)$$

Recalling the chain rule and vector relationship we can write (3.18) at the form,

$$\rho \frac{DV}{Dt} = \frac{\partial(\rho u)}{\partial t} - u\left[\frac{\partial \rho}{\partial t} + \nabla.(\rho V)\right] + \nabla.(\rho UV), \qquad (3.19)$$

The second term of the right hand side in bracket is the expression of continuity equation as is expressed in equation (3.8) which implies that will be zero. Therefore, we will have:

$$\rho \frac{DV}{Dt} = \frac{\partial(\rho u)}{\partial t} + \nabla.(\rho UV), \qquad (3.20)$$

Substitute equation (3.19) into equation (3.16) we will have:

$$\frac{\partial(\rho u)}{\partial t} + \nabla.(\rho uV) = -\frac{\partial p}{\partial x} + \frac{\partial \tau_{xx}}{\partial x} + \frac{\partial \tau_{yx}}{\partial y} + \frac{\partial \tau_{zx}}{\partial z} + \rho f_x,$$

$$\frac{\partial(\rho v)}{\partial t} + \nabla.(\rho vV) = -\frac{\partial p}{\partial y} + \frac{\partial \tau_{xy}}{\partial x} + \frac{\partial \tau_{yy}}{\partial y} + \frac{\partial \tau_{zy}}{\partial z} +$$

$$\rho f_y, \qquad\qquad (3.21)$$

$$\frac{\partial(\rho w)}{\partial t} + \nabla.(\rho wV) = -\frac{\partial p}{\partial z} + \frac{\partial \tau_{xz}}{\partial x} + \frac{\partial \tau_{yz}}{\partial y} + \frac{\partial \tau_{zz}}{\partial z} + \rho f_z,$$

For Newtonian Fluids Shear stress is proportional to the deformation rate and the constant of proportionality is called the viscosity, i.e $\tau = \mu \nabla V$

$$\tau = \begin{pmatrix} \tau_{xx} & \tau_{xy} & \tau_{xz} \\ \tau_{yx} & \tau_{yy} & \tau_{yz} \\ \tau_{zx} & \tau_{zy} & \tau_{zz} \end{pmatrix} = \begin{pmatrix} 2\mu\frac{\partial u}{\partial x} + \lambda \nabla . V & \mu\left(\frac{\partial u}{\partial y} + \frac{\partial v}{\partial x}\right) & \mu\left(\frac{\partial u}{\partial z} + \frac{\partial w}{\partial x}\right) \\ \mu\left(\frac{\partial v}{\partial x} + \frac{\partial u}{\partial y}\right) & 2\mu\frac{\partial v}{\partial y} + \lambda \nabla . V & \mu\left(\frac{\partial v}{\partial z} + \frac{\partial w}{\partial y}\right) \\ \mu\left(\frac{\partial w}{\partial x} + \frac{\partial u}{\partial z}\right) & \mu\left(\frac{\partial w}{\partial y} + \frac{\partial v}{\partial z}\right) & 2\mu\frac{\partial w}{\partial z} + \lambda \nabla . V \end{pmatrix}, \qquad (3.22)$$

where ∇V is the velocity gradient, μ is viscous λ is bulk viscosity coefficient which has the following relationship with λ: $\lambda = -\frac{2}{3}\mu$ only if the flow is incompressible.

Substituting equation (3.18) into equation (3.17) we will have momentum equation as follows:

$$\left. \begin{aligned} \rho\left(\frac{\partial u}{\partial t} + u\frac{\partial u}{\partial x} + v\frac{\partial u}{\partial y} + w\frac{\partial u}{\partial z}\right) &= -\frac{\partial p}{\partial x} + \mu\nabla^2 u + \rho f_x , \\ \rho\left(\frac{\partial v}{\partial t} + u\frac{\partial u}{\partial x} + v\frac{\partial v}{\partial y} + w\frac{\partial v}{\partial z}\right) &= -\frac{\partial p}{\partial y} + \mu\nabla^2 v + \rho f_y , \\ \rho\left(\frac{\partial u}{\partial t} + u\frac{\partial w}{\partial x} + v\frac{\partial w}{\partial y} + w\frac{\partial w}{\partial z}\right) &= -\frac{\partial p}{\partial z} + \mu\nabla^2 u + \rho f_z, \end{aligned} \right\} \qquad (3.23)$$

Where ∇^2 is laplace operator

$$\nabla^2 \equiv \frac{\partial^2}{\partial x^2} + \frac{\partial^2}{\partial y^2} + \frac{\partial^2}{\partial z^2} ,$$

In a vector form can be written as:

$$\rho\left(\frac{\partial V}{\partial t} + (V.\nabla)V\right) = -\nabla p + \mu\nabla^2 V + \vec{f} . \qquad (3.24)$$

In cylindrical polar coordinates,

r- component

$$\rho\left(\frac{\partial u_r}{\partial t} + u_r\frac{\partial u_r}{\partial r} + \frac{u_\theta}{r}\frac{\partial u_r}{\partial \theta} - \frac{u^2_\theta}{r}\right) = -\frac{\partial p}{\partial r} + \rho g_r + \mu\left(\frac{1}{r}\frac{\partial}{\partial r}\left(r\frac{\partial u_r}{\partial r}\right) + \frac{1}{r}\frac{\partial u_r}{\partial r} - \frac{u_r}{r^2} + \frac{1}{r^2}\frac{\partial^2 u_r}{\partial \theta^2} + \right.$$
$$\left. \frac{\partial^2 u_r}{\partial z^2} - \frac{2}{r^2}\frac{\partial u_\theta}{\partial \theta}\right), \qquad (3.25)$$

θ- component

$$\rho\left(\frac{\partial u_\theta}{\partial t} + u_r\frac{\partial u_\theta}{\partial r} + \frac{u_\theta u_r}{r} + \frac{u_\theta}{r}\frac{\partial u_\theta}{\partial \theta} + u_z\frac{\partial u_\theta}{\partial z}\right) = -\frac{1}{r}\frac{\partial p}{\partial \theta} + \rho g_\theta + \mu\left(\frac{1}{r}\frac{\partial}{\partial r}\left(r\frac{\partial u_\theta}{\partial r}\right) + \frac{1}{r}\frac{\partial u_\theta}{\partial r} - \frac{u_\theta}{r^2} + \right.$$
$$\frac{1}{r^2}\frac{\partial^2 u_\theta}{\partial \theta^2} + \frac{\partial^2 u_\theta}{\partial z^2} + $$
$$\left. \frac{2}{r^2}\frac{\partial u_r}{\partial \theta}\right), \qquad (3.26)$$

z- component

$$\rho\left(\frac{\partial u_z}{\partial t} + u_r\frac{\partial u_z}{\partial r} + \frac{u_\theta}{r} + \frac{u_\theta}{r}\frac{\partial u_z}{\partial \theta} + u_z\frac{\partial u_z}{\partial z}\right) = -\frac{\partial p}{\partial z} + \rho g_z + \mu\left(\frac{1}{r}\frac{\partial}{\partial r}\left(r\frac{\partial u_z}{\partial r}\right) + \frac{1}{r}\frac{\partial u_z}{\partial r} + \frac{1}{r^2}\frac{\partial^2 u_z}{\partial \theta^2} +$$

$$\frac{\partial^2 u_z}{\partial z^2}\right), \tag{3.27}$$

3.2.3 Energy equation

The thermodynamics first law will be applied which stipulates that "The internal energy (E) is a state variable that exists in any thermodynamic system in equilibrium state the difference in heat transfer into the system and work done by the system between any two equilibrium states is equal to the change in internal energy."

$$\frac{dE}{dt} = \frac{dW}{dt} + \frac{dQ}{dt}, \tag{3.28}$$

Where;

$\frac{dE}{dt}$ is the rate at which total energy, including internal and kinetic energy changes.

$\frac{dW}{dt}$ is the rate of work done.

$\frac{dQ}{dt}$ is the net heat flux.

Surface forces and body forces may cause work to be done on the system. The work done by a body force acting on a moving fluid element is given by:

$$\frac{dW_b}{dt} = \rho\vec{f}.V(dxdydz), \tag{3.29}$$

For surface forces work done is obtained by taking the product of velocity and corresponding surface force components.

$$\frac{dW_s}{dt} = \left[-\left(\frac{\partial(up)}{\partial x} + \frac{\partial(vp)}{\partial y} + \frac{\partial(wp)}{\partial z}\right) + \left(\frac{\partial(u\tau_{xx})}{\partial x} + \frac{\partial(u\tau_{yx})}{\partial y} + \frac{\partial(u\tau_{zx})}{\partial z}\right) + \left(\frac{\partial(v\tau_{yx})}{\partial x} + \frac{\partial(u\tau_{yy})}{\partial y} + \frac{\partial(u\tau_{zy})}{\partial z}\right) +$$

$$\left(\frac{\partial(w\tau_{zx})}{\partial x} + \frac{\partial(w\tau_{zy})}{\partial y} + \frac{\partial(w\tau_{zz})}{\partial z}\right)\right]dxdydz, \tag{3.30}$$

Therefore, the net rate of work done on the moving fluid element is given by:

$$\frac{dW}{dt} = \left[-\left(\frac{\partial(up)}{\partial x} + \frac{\partial(vp)}{\partial y} + \frac{\partial(wp)}{\partial z}\right) + \left(\frac{\partial(u\tau_{xx})}{\partial x} + \frac{\partial(u\tau_{yx})}{\partial y} + \frac{\partial(u\tau_{zx})}{\partial z}\right) + \left(\frac{\partial(v\tau_{yx})}{\partial x} + \frac{\partial(u\tau_{yy})}{\partial y} +$$

$$\frac{\partial(u\tau_{zy})}{\partial z}\right) + \left(\frac{\partial(w\tau_{zx})}{\partial x} + \frac{\partial(w\tau_{zy})}{\partial y} + \frac{\partial(w\tau_{zz})}{\partial z}\right)\right]dxdydz +$$

$$\rho\vec{f}.V(dxdydz) \tag{3.31}$$

Because of volumetric heating, the net heat flux added to the fluid element is:

$$\frac{dQ_v}{dt} = \rho\dot{q}\,dxdydz, \tag{3.32}$$

Where

$\dot{q}$ is rate of volumetric heat per unit mass

Thermal conduction contributes a net heat flux to the fluid element by:

$$\frac{dQ_c}{dt} = -\left(\frac{\partial\dot{q}_x}{\partial x} + \frac{\partial\dot{q}_y}{\partial y} + \frac{\partial\dot{q}_z}{\partial z}\right)dxdydz, \tag{3.33}$$

By summing equation (3.28) and equation (3.29) we will get net heat flux that:

$$\frac{dQ}{dt} = \left[\rho\dot{q} - \left(\frac{\partial\dot{q}_x}{\partial x} + \frac{\partial\dot{q}_y}{\partial y} + \frac{\partial\dot{q}_z}{\partial z}\right)\right]dxdydz, \tag{3.34}$$

The thermal conduction is proportional to the local temperature gradient, according to Fourier's law of heat conduction. Therefore, we will have:

$$\dot{q}_x = -k\frac{\partial T}{\partial x}, \dot{q}_y = -k\frac{\partial T}{\partial y} \text{ and } \dot{q}_z = -k\frac{\partial T}{\partial z}$$

Where

T = temperature and

k is the fluid's thermal conductivity.

Therefore, equation (3.27) can be written as;

$$\frac{dQ}{dt} = \left[\rho\dot{q} + \frac{\partial}{\partial x}\left(k\frac{\partial T}{\partial x}\right) + \frac{\partial}{\partial y}\left(k\frac{\partial T}{\partial y}\right) + \frac{\partial}{\partial z}\left(k\frac{\partial T}{\partial z}\right)\right]dxdydz, \tag{3.35}$$

The fluid element's total energy is given by:

$$\frac{dE}{dt} = \rho\frac{D}{Dt}\left(e + \frac{V^2}{2}\right)dxdydz, \tag{3.36}$$

Where e is the fluid element's internal energy per unit mass

$\frac{V^2}{2}$ is the fluid element's kinetic energy per unit mass due to motion.

After the equations (3.31), (3.35) and (3.36) have been substituted and simplified in equation (3.21) we will have:

$$\rho \frac{D}{Dt}\left(e + \frac{V^2}{2}\right) = \left[\rho\dot{q} + \rho\dot{q} + \frac{\partial}{\partial x}\left(k\frac{\partial T}{\partial x}\right) + \frac{\partial}{\partial y}\left(k\frac{\partial T}{\partial y}\right) + \frac{\partial}{\partial z}\left(k\frac{\partial T}{\partial z}\right)\right] + \left[-\left(\left(\frac{\partial(up)}{\partial x} + \frac{\partial(vp)}{\partial y} + \right.\right.\right.$$

$$\left.\frac{\partial(wp)}{\partial z}\right) + \left(\frac{\partial(u\tau_{xx})}{\partial x} + \frac{\partial(u\tau_{yx})}{\partial y} + \frac{\partial(u\tau_{zx})}{\partial z}\right) + \left(\frac{\partial(v\tau_{yx})}{\partial x} + \frac{\partial(u\tau_{yy})}{\partial y} + \frac{\partial(u\tau_{zy})}{\partial z}\right) + \left(\frac{\partial(w\tau_{zx})}{\partial x} + \frac{\partial(w\tau_{zy})}{\partial y} + \right.$$

$$\left.\left.\left.\frac{\partial(w\tau_{zz})}{\partial z}\right)\right) + \right.$$

$$\left. \rho\vec{f}.V\right], \tag{3.37}$$

Multiply equation (3.17) by u, v and w and finding the sum of those three equation we will obtain the following result:

$$\rho\frac{D(V^2/2)}{Dt} = \left[-\left(u\frac{\partial p}{\partial x} + v\frac{\partial p}{\partial y} + w\frac{\partial p}{\partial z}\right) + u\left(\frac{\partial\tau_{xx}}{\partial x} + \frac{\partial\tau_{yx}}{\partial y} + \frac{\partial\tau_{zx}}{\partial z}\right) + v\left(\frac{\partial\tau_{xy}}{\partial x} + \frac{\partial\tau_{yy}}{\partial y} + \frac{\partial\tau_{zy}}{\partial z}\right) + \right.$$

$$w\left(\frac{\partial\tau_{xz}}{\partial x} + \frac{\partial\tau_{yz}}{\partial y} + \frac{\partial\tau_{zz}}{\partial z}\right) + \rho\left(uf_x + vf_y + \right.$$

$$\left.\left. wf_z\right)\right], \tag{3.38}$$

Where $V^2 = u^2 + v^2 + w^2$

After subtracting mechanical energy (potential and kinetic energy) equation (3.38) from the total energy equation (3.37), the equation (3.39) equals the thermal energy in the fluid element.

$$\rho\frac{De}{Dt} = \rho\dot{q} + \rho\dot{q} + \frac{\partial}{\partial x}\left(k\frac{\partial T}{\partial x}\right) + \frac{\partial}{\partial y}\left(k\frac{\partial T}{\partial y}\right) + \frac{\partial}{\partial z}\left(k\frac{\partial T}{\partial z}\right) - p\left(\frac{\partial u}{\partial x} + \frac{\partial v}{\partial y} + \frac{\partial w}{\partial z}\right) + \tau_{xx}\frac{\partial u}{\partial x} + \tau_{yx}\frac{\partial u}{\partial y} + $$

$$\tau_{zx}\frac{\partial u}{\partial z} + \tau_{xy}\frac{\partial v}{\partial x} + \tau_{yy}\frac{\partial v}{\partial y} + \tau_{zy}\frac{\partial v}{\partial z} + \tau_{xz}\frac{\partial w}{\partial x} + \tau_{yz}\frac{\partial w}{\partial y} + $$

$$\tau_{zz}\frac{\partial w}{\partial z} , \tag{3.39}$$

The following result is obtained after substituting the normal and shear stresses relations equation (3.22) also, the Navier hypothesis into the equation of thermal energy.

$$\rho\frac{De}{Dt} = \rho\dot{q} + \frac{\partial}{\partial x}\left(k\frac{\partial T}{\partial x}\right) + \frac{\partial}{\partial y}\left(k\frac{\partial T}{\partial y}\right) + \frac{\partial}{\partial z}\left(k\frac{\partial T}{\partial z}\right) - p\left(\frac{\partial u}{\partial x} + \frac{\partial v}{\partial y} + \frac{\partial w}{\partial z}\right) + \mu\phi , \tag{3.40}$$

Where

$$\phi = 2\left(\frac{\partial u}{\partial x}\right)^2 + 2\left(\frac{\partial v}{\partial y}\right)^2 + 2\left(\frac{\partial w}{\partial z}\right)^2 - \frac{2}{3}\left(\frac{\partial u}{\partial x} + \frac{\partial v}{\partial y} + \frac{\partial w}{\partial z}\right)^2 + \left(\frac{\partial u}{\partial y} + \frac{\partial v}{\partial x}\right)^2 + \left(\frac{\partial u}{\partial z} + \frac{\partial w}{\partial x}\right)^2 + \left(\frac{\partial v}{\partial z} + \right.$$

$$\left.\frac{\partial w}{\partial y}\right)^2$$

ϕ is the dissipation function representing the transformation created by friction between moving fluid layers into thermal energy.

Thermodynamic relations are introduced into the thermal energy equation we obtain:

$$\rho c_p \frac{DT}{Dt} = \rho \dot{q} + \frac{\partial}{\partial x}\left(k\frac{\partial T}{\partial x}\right) + \frac{\partial}{\partial y}\left(k\frac{\partial T}{\partial y}\right) + \frac{\partial}{\partial z}\left(k\frac{\partial T}{\partial z}\right) - p\left(\frac{\partial u}{\partial x} + \frac{\partial v}{\partial y} + \frac{\partial w}{\partial z}\right) +$$

$$\mu\phi \,, \qquad\qquad (3.41)$$

c_p is specific heat at constant pressure

Also $\frac{\partial u}{\partial x} + \frac{\partial v}{\partial y} + \frac{\partial w}{\partial z} = 0$

Hence the energy equation in non-conservative form becomes:

$$\rho c_p \frac{DT}{Dt} = \frac{\partial}{\partial x}\left(k\frac{\partial T}{\partial x}\right) + \frac{\partial}{\partial y}\left(k\frac{\partial T}{\partial y}\right) + \frac{\partial}{\partial z}\left(k\frac{\partial T}{\partial z}\right) + \mu\phi \,. \qquad\qquad (3.42)$$

Introducing the substantial derivative into equation (3.42) we will obtain:

$$\rho c_p \left(\frac{\partial T}{\partial t} + u\frac{\partial T}{\partial x} + v\frac{\partial T}{\partial y} + w\frac{\partial T}{\partial z}\right) = \frac{\partial}{\partial x}\left(k\frac{\partial T}{\partial x}\right) + \frac{\partial}{\partial y}\left(k\frac{\partial T}{\partial y}\right) + \frac{\partial}{\partial z}\left(k\frac{\partial T}{\partial z}\right) + \mu\phi \,. \quad (3.43)$$

In vector form energy equation can be written as:

$$\rho c_p \left(\frac{\partial T}{\partial t} + (V.\nabla)T\right) = k\nabla^2 T + \mu\phi \,. \qquad\qquad (3.44)$$

In cylindrical polar:

$$c_p \left(\frac{\partial T}{\partial t} + u_r\frac{\partial T}{\partial r} + \frac{u_\theta}{r}\frac{\partial T}{\partial \theta} + u_z\frac{\partial T}{\partial z}\right) = k\left(\frac{1}{r}\frac{\partial}{\partial r}\left(r\frac{\partial T}{\partial r}\right) + \frac{1}{r^2}\frac{\partial^2 T}{\partial \theta^2} + \frac{\partial^2 T}{\partial z^2}\right) + \; 2\mu\left\{\left(\frac{\partial u_r}{\partial r}\right)^2 + \right.$$

$$\left.\left[\frac{1}{r}\left(\frac{\partial u_\theta}{\partial \theta} + u_r\right)\right]^2 + \left(\frac{\partial u_z}{\partial z}\right)^2\right\} + \mu\left\{\left(\frac{\partial u_\theta}{\partial z} + \frac{1}{r}\frac{\partial u_z}{\partial \theta}\right)^2 + \left(\frac{\partial u_\theta}{\partial z} + \frac{1}{r}\frac{\partial u_z}{\partial \theta}\right)^2 + \left(r\frac{\partial}{\partial r}\left(\frac{u_\theta}{r}\right) + \right.\right.$$

$$\left.\left.\frac{1}{r}\frac{\partial u_r}{\partial \theta}\right)^2\right\}. \qquad\qquad (3.45)$$

3.3   Model equations

During the flow we consider incompressible laminar flow in one direction (r) means that the flow in (z) and (θ) are very small in such a way that are negligible. Newtonian nanofluid having Copper and Alumina nanoparticles passes through the porous pipe with partial slip condition at the wall (Fig. 7).

$$\mu_f \frac{\partial u}{\partial r} = \beta u \qquad u = 0 \quad v = V \qquad -k_{nf} \frac{\partial T}{\partial r} = h(T - T_a) \quad T = T_a$$
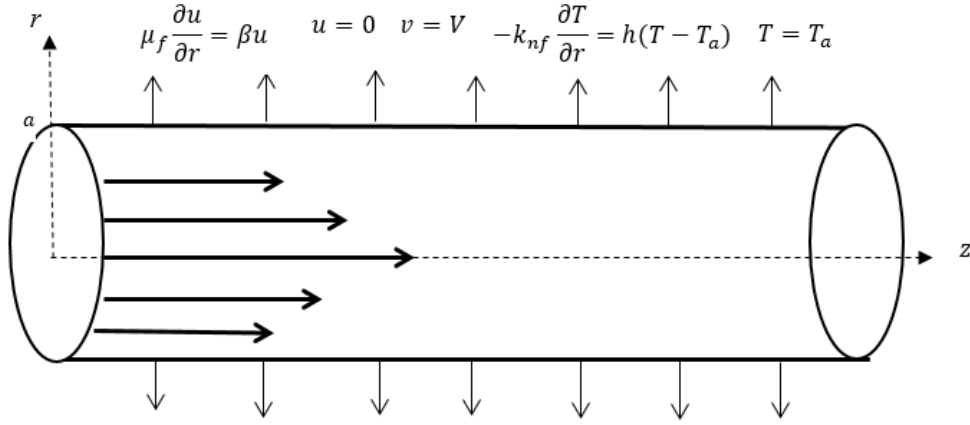
Figure 7: The schematic flow of the problem

The flow is governed by the following equations:

$$\frac{\partial u}{\partial z} = 0 , \tag{3.46}$$

$$\rho_{nf} \left(\frac{\partial u}{\partial \bar{t}} + V \frac{\partial u}{\partial r} \right) = -\frac{\partial p}{\partial z} + \mu_{nf} \frac{\partial^2 u}{\partial r^2} , \tag{3.47}$$

$$(\rho c_p)_{nf} \left(\frac{\partial T}{\partial \bar{t}} + V \frac{\partial T}{\partial r} \right) = k_{nf} \frac{\partial^2 T}{\partial r^2} + \mu_{nf} \left(\frac{\partial u}{\partial r} \right)^2 , \tag{3.48}$$

The nanofluid constants are defined as,

$$\left. \begin{aligned} \rho_{nf} &= (1 - \varphi)\rho_f + \varphi \rho_s, \\ \alpha_{nf} = \frac{k_{nf}}{(\rho c_p)_{nf}}, \qquad \tau &= \frac{(\rho c_p)_s}{(\rho c_p)_f}, \quad \frac{k_{nf}}{k_f} = \frac{(k_s + 2k_f) - 2\varphi(k_f - k_s)}{(k_s + 2k_f) + \varphi(k_f - k_s)}, \\ (\rho c_p)_{nf} = (1 - \varphi)(\rho c_p)_f &+ \varphi(\rho c_p)_s, \mu_{nf} = \frac{\mu_f}{(1 - \varphi)^{2.5}}. \end{aligned} \right\} \tag{3.49}$$

where, ρ_f and ρ_s are the fluid and solid fraction's reference density, k_s and k_f are the thermal conductivity of the solid and fluid volume fraction respectively, φ is the solid volume fraction of nanoparticles, α_{nf} is the thermal diffusivity of nanofluid, $(\rho c_p)_s$ and $(\rho c_p)_f$ is heat capacity of solid and fluid respectively.

The initial condition and boundary condition are given in (3.50) to (3.52)

$$u(r, 0) = 0, \ T(r, 0) = T_a , \quad where \ 0 \le r \le a \tag{3.50}$$

$$\mu_f \frac{\partial u}{\partial r}(0,\bar{t}),= -\beta u(0,\bar{t}), \qquad T(0,\bar{t}) = T_a, \tag{3.51}$$

$$u(a,\bar{t}) = 0, \qquad -k_{nf}\frac{\partial T}{\partial r}T(a,\bar{t}) = h(T(a,\bar{t}) - T_a). \tag{3.52}$$

The following dimensionless variables and parameters are introduced:

$$
\left.
\begin{aligned}
&\theta = \frac{T-T_0}{T_a-T_0}, \quad W = \frac{u}{V}, \quad \eta = \frac{r}{a}, \quad t = \frac{\bar{t}v_f}{a^2}, \quad v_f = \frac{\mu_f}{\rho_f}, \lambda = \frac{\mu_f}{\beta a}, \\
&Re = \frac{Va}{v_f}, P = \frac{ap}{\mu_f V}, A = -\frac{\partial p}{\partial z}, \tau = \frac{(\rho c_p)_s}{(\rho c_p)_f} \quad , Z = \frac{z}{a}, \\
&Ec = \frac{V^2}{c_{pf}(T_a-T_0)}, Pr = \frac{\mu_f c_{pf}}{k_f}, C_1 = \frac{k_s+2k_f-2\varphi(k_f-k_s)}{k_s+2k_f+\varphi(k_f-k_s)}, Bi = \frac{ha}{k_f}.
\end{aligned}
\right\} \tag{3.53}
$$

Converting governing equations into the dimensionless form, we get

Momentum equation:

$$
\left.
\begin{aligned}
W = \frac{u}{V} &\Rightarrow \partial W = \frac{1}{V}\partial u \Rightarrow \partial u = V\partial W \Rightarrow \partial^2 u = V\partial W^2, \\
t = \frac{\bar{t}v_f}{a^2} &\Rightarrow \partial t = \frac{v_f}{a^2}\partial\bar{t} \Rightarrow \partial\bar{t} = \frac{a^2}{v_f}\partial t, \\
P = \frac{ap}{\mu_f V} &\Rightarrow \partial P = \frac{a}{\mu_f V}\partial p \Rightarrow \partial p = \frac{\mu_f V\partial P}{a}, \\
\eta = \frac{r}{a} &\Rightarrow \partial\eta = \frac{1}{a}\partial r \Rightarrow \partial r = a\partial\eta \Rightarrow \partial r^2 = a^2\partial\eta^2 \\
Z = \frac{z}{a} &\Rightarrow \partial Z = \frac{1}{a}\partial z \Rightarrow \partial z = a\partial Z
\end{aligned}
\right\} \tag{3.54}
$$

Substituting equation (3.54) into equation (3.47) the momentum equation will be:

$$\rho_{nf}\frac{v_f V}{a^2}\cdot\frac{\partial W}{\partial t} + \rho_{nf}\frac{V^2}{a}\cdot\frac{\partial W}{\partial\eta}$$

$$= -\frac{\mu_f V}{a}\cdot\frac{\partial P}{\partial Z} + \frac{\mu_{nf}V}{a^2}\cdot\frac{\partial^2 W}{\partial\eta^2}, \tag{3.55}$$

Multiply throughout the equation (3.55) by $\frac{a^2}{\rho_{nf}v_f V}$

$$\frac{\partial W}{\partial t} + \frac{av}{v_f}\cdot\frac{\partial W}{\partial\eta} = -\frac{\mu_f}{\rho_{nf}v_f}\cdot\frac{\partial P}{\partial Z} + \frac{\mu_{nf}}{v_f\rho_{nf}}\cdot\frac{\partial^2 W}{\partial\eta^2}, \tag{3.56}$$

Also using definition in equation (3.49) and (3.53) then momentum equation (3.56) will be as follows:

$$\frac{\partial W}{\partial t} = \frac{A}{1-\varphi+\varphi\rho_s/\rho_f} + \frac{1}{(1-\varphi)^{2.5}(1-\varphi+\varphi\rho_s/\rho_f)}\frac{\partial^2 W}{\partial\eta^2} - Re\frac{\partial W}{\partial\eta} . \tag{3.57}$$

Energy equation:

$$\theta = \frac{T-T_0}{T_w-T_0} \Rightarrow T = \theta(T_w-T_0)+T_0 \Rightarrow \partial T = \partial\theta(T_w-T_0) \Rightarrow \partial^2 T$$
$$= (T_w-T_0)\partial^2\theta \tag{3.58}$$

Use equation (3.54) and (3.58) and substitute into equation (3.48) we will obtain:

$$(\rho c_p)_{nf}\frac{(T_w-T_0)v_f}{a^2}\cdot\frac{\partial\theta}{\partial t} + (\rho c_p)_{nf}.V\frac{(T_w-T_0)}{a}\cdot\frac{\partial\theta}{\partial\eta} = k_{nf}\frac{(T_w-T_0)}{a^2}\cdot\frac{\partial^2\theta}{\partial\eta^2} +$$
$$\mu_{nf}\frac{V^2}{a^2}\cdot\left(\frac{\partial W}{\partial\eta}\right)^2, \tag{3.59}$$

Multiply by $\dfrac{a^2}{(\rho c_p)_{nf}(T_w-T_0)v_f}$ in equation (3.59) throughout we obtain:

$$\frac{\partial\theta}{\partial t} + \frac{va}{v_f}\frac{\partial\theta}{\partial\eta} = k_{nf}\frac{1}{v_f(\rho c_p)_{nf}}\cdot\frac{\partial^2\theta}{\partial\eta^2}$$
$$+ \frac{\mu_{nf}V^2}{(\rho c_p)_{nf}(T_w-T_0)v_f}\cdot\left(\frac{\partial W}{\partial\eta}\right)^2, \tag{3.60}$$

Also using definition in equation (3.49) and (3.53) the energy equation (3.60) we will be as follows:

$$\frac{\partial\theta}{\partial t} + Re\frac{\partial\theta}{\partial\eta} = c_1\frac{k_f}{v_f(1-\varphi)(\rho c_p)_f+\varphi(\rho c_p)_s}\cdot\frac{\partial^2\theta}{\partial\eta^2} +$$
$$\frac{\mu_f V^2}{(1-\varphi)(\rho c_p)_f+\varphi(\rho c_p)_s(T_w-T_0)v_f(1-\varphi)^{2.5}}\cdot\left(\frac{\partial W}{\partial\eta}\right)^2, \tag{3.61}$$

Multiply by $\dfrac{\frac{1}{(\rho c_p)_f}}{\frac{1}{(\rho c_p)_f}}$ the left hand side of equation (3.61) we obtain:

$$\frac{\partial\theta}{\partial t} + Re\frac{\partial\theta}{\partial\eta} = c_1\frac{k_f}{(\rho c_p)_f v_f\left((1-\varphi)+\varphi\frac{(\rho c_p)_s}{(\rho c_p)_f}\right)}\cdot\frac{\partial^2\theta}{\partial\eta^2} + \frac{\rho_f V^2}{(\rho c_p)_f(T_w-T_0)(1-\varphi)^{2.5}\left((1-\varphi)+\varphi\frac{(\rho c_p)_s}{(\rho c_p)_f}\right)}\cdot\left(\frac{\partial W}{\partial\eta}\right)^2, \tag{3.62}$$

Opening the bracket of the term $(\rho c_p)_f$ we will have:

$$\frac{\partial \theta}{\partial t} + Re \frac{\partial \theta}{\partial \eta} = c_1 \frac{k_f}{\rho_f c_{pf} v_f \left((1-\varphi)+\varphi \frac{(\rho c_p)_s}{(\rho c_p)_f} \right)} \cdot \frac{\partial^2 \theta}{\partial \eta^2} + \frac{\rho_f V^2}{\rho_f c_{pf}(T_w-T_0)(1-\varphi)^{2.5}\left((1-\varphi)+\varphi \frac{(\rho c_p)_s}{(\rho c_p)_f} \right)} \cdot \left(\frac{\partial W}{\partial \eta}\right)^2 , \quad (3.63)$$

Using the definition (3.53) into equation (3.63) we will have;

$$\frac{\partial \theta}{\partial t} = c_1 \frac{1}{Pr(1-\varphi+\varphi\tau)} \frac{\partial^2 \theta}{\partial \eta^2} + \frac{E_C}{(1-\varphi)^{2.5}(1-\varphi+\varphi\tau)} \left(\frac{\partial W}{\partial \eta}\right)^2 -$$
$$Re \frac{\partial \theta}{\partial \eta} . \qquad\qquad (3.64)$$

And initial and boundary condition will be as follows:

$$\left.\begin{array}{l}
At \quad \bar{t} \le 0 \;,\; t = \dfrac{\bar{t}}{T} = 0 \qquad and \quad T > 0 \;,\; \bar{t} > 0 \\[2mm]
At \quad u \le 0 \;,\; W = \dfrac{u}{V} = 0 \qquad and \quad u = V \;,\; W = \dfrac{V}{V} = 1, \\[2mm]
At\; T = T_a \;,\; \theta = \dfrac{T-T_0}{T_a-T_0} = \dfrac{T_a-T_0}{T_a-T_0} = 1 \quad and \quad T = T_0 \;, \quad \theta = \dfrac{T_0-T_0}{T_a-T_0} = 0, \\[2mm]
At\; r = -a, \quad \eta = \dfrac{r}{a} = -\dfrac{a}{a} = -1\; and\; r = a, \quad \eta = \dfrac{r}{a} = \dfrac{a}{a} = 1,
\end{array}\right\} 3.65$$

Substituting equation (3.53), (3.54) and (3.58) into (3.65) we obtain:

$$W(\eta, 0) = 0, \;\; \theta(\eta, 0) = 0 \;, \qquad\qquad (3.68)$$

$$\frac{\partial W}{\partial \eta}(0, t) = -\frac{\beta a}{\mu_f} W(0, t), \qquad \theta(0, t) = 0 \;, \qquad\qquad (3.69)$$

$$W(1, t) = 0, \qquad \frac{\partial \theta}{\partial \eta}(1, t) = -mBi\theta(1, t), \qquad\qquad (3.70)$$

C_f and Nu are in (3.71)- (3.72)

$$C_f = \frac{a\tau_w}{\mu_0 V}, \qquad\qquad Nu = \frac{aq_w}{k_f(T_w-T_0)}, \qquad\qquad (3.71)$$

where q_w and τ_w is given by (3.72):

$$\tau_w = -\mu_{nf} \left.\frac{\partial u}{\partial r}\right|_{r=a}, \quad q_w = -k_{nf} \left.\frac{\partial T}{\partial r}\right|_{r=a}, \qquad\qquad (3.72)$$

25

Substituting τ_w and q_w from (3.72) into (3.71) and using the dimensionless variables with manipulations results into (3.73):

$$C_f = -\frac{1}{(1-\varphi)^{2.5}}\frac{\partial W}{\partial \eta}$$

$$\left.\begin{array}{c}\\\\\end{array}\right\} \quad \text{at} \quad \eta = 1 \qquad (3.73)$$

$$Nu = c_1 \frac{\partial \theta}{\partial \eta}$$

3.4   Numerical Procedure

3.4.1   Semi-discretization method (Method of lines)

Method of lines is a method for solving partial differential equations in which the differential equation's space variable is discretized (ΔW or $\Delta \eta$) but the time variable is not. The concept is to discretize only along spatial coordinates, which is known as semi-discretization. By discretizing in space while keeping time continuous, an ODE system is obtained where a numerical approach for solving ordinary equations with initial values can be used (Morton & Mayers, 2005). We will use Fig. 8.

Figure 8: Mesh grid

The horizontal axis represents spatial variables, while the vertical axis represents time variables in this rectangular mesh grid. The difference analogs of the partial derivatives are given in (3.74) to (3.77). The method is used to discretize (3.57), (3.64) and (3.68) to (3.70) which result in (3.78) to (3.81).

$$\frac{\partial \theta}{\partial \eta} = \frac{\theta_{i+1} - \theta_{i-1}}{2\Delta \eta}, \qquad (3.74)$$

$$\frac{\partial W}{\partial \eta} = \frac{W_{i+1} - W_{i-1}}{2\Delta\eta},$$

(3.75)

$$\frac{\partial^2\theta}{\partial\eta^2} = \frac{\theta_{i+1} - 2\theta_i + \theta_{i-1}}{\Delta\eta^2},$$

(3.76)

$$\frac{\partial^2 W}{\partial\eta^2} = \frac{W_{i+1} - 2W_i + W_{i-1}}{\Delta\eta^2},$$

(3.77)

Then, the discretization of equation (3.57) and (3.64) we will have the model equation is as follows:

$$\frac{\partial W}{\partial t} = \frac{A}{1-\varphi+\varphi\rho_s/\rho_f} + \frac{1}{(1-\varphi)^{2.5}(1-\varphi+\varphi\rho_s/\rho_f)}\left(\frac{W_{i+1}-2W_i+W_{i-1}}{\Delta\eta^2}\right) - Re\left(\frac{W_{i+1}-W_{i-1}}{2\Delta\eta}\right),$$

(3.78)

$$\frac{\partial\theta}{\partial t} = c_1\frac{1}{Pr(1-\varphi+\varphi\tau)}\left(\frac{\theta_{i+1}-2\theta_i+\theta_{i-1}}{\Delta\eta^2}\right) + \frac{E_C}{(1-\varphi)^{2.5}(1-\varphi+\varphi\tau)}\left(\frac{W_{i+1}-W_{i-1}}{2\Delta\eta}\right)^2 - Re\left(\frac{\theta_{i+1}-\theta_{i-1}}{2\Delta\eta}\right),$$

(3.79)

Here initial and boundary conditions are:

$$W_i(0) = \theta_i(0) = 0, \qquad 1 \le i \le N+1,$$

(3.80)

$$W_i = \frac{-\lambda W_2}{\Delta\eta - \lambda}, \quad \varphi_1 = 0, \qquad W_{N+1} = 1, \quad \theta_{N+1} = \varphi_N(1 - mBi\Delta\eta),$$

(3.81)

Where $W_i(t)$ and $\theta_i(t)$ be the approximation of $W(\eta_i, t)$ and $\theta(\eta_i, t)$ as shown above.

Considering the equation (3.78) - (3.81) that may be solved simultaneously using a computer code in MATLAB.

3.4.2 Material properties

When heat is applied to a substance, it exhibits certain characteristics which is called thermophysical characteristics for our case we are going to consider density and specific heat capacity of water, copper, and alumina shown in Table 1.

27

Table 1: Nanoparticle and fluid phase (water) and thermophysical characteristics

| Physical properties	Fluid phase (water)	Cu	Al_2O_3
c_p (J/kgK)	4179	385	765
ρ (kg/m^3)	997.1	8933	3970

CHAPTER FOUR

RESULTS AND DISCUSSION

## 4.1   Effects of parameter variation on velocity and temperature profiles

The numerical results and discussion are presented in this chapter. Water-based nanofluids of two types Copper and Alumina are considered in this study while variation of different parameters was taken into consideration while Pr is fixed at 6.2. MATLAB codes for discretized equations (3.77) - (3.78) were written and implemented to produce graph. Then produced graph has four line colours which are black, green, blue and red this lines indicates the value if parameters from the smallest value to the highest value respectively.

Figure 9, displays that, Alumina has a greater nanofluid velocity profile than Copper since density of Copper is high and specific heat capacity of Alumina being higher than that of Copper.
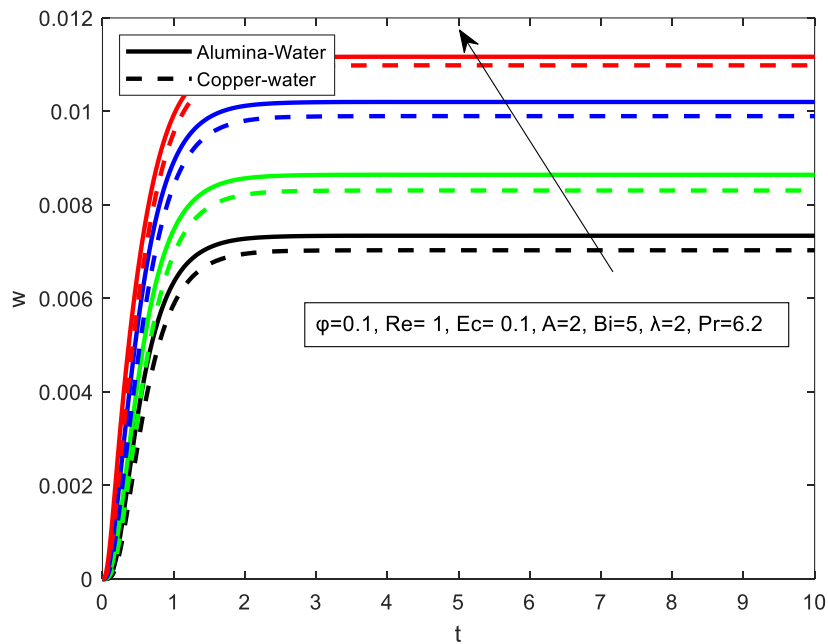

Figure 9: Copper and Alumina nanofluid velocity profile

Figure 10 and Fig. 11, shows the relationship of nanoparticle fraction in velocity and temperature, it is observed that as the volume of nanoparticle increases, velocity and temperature at the wall drops compared to the center of the pipes may be when nanoparticles is added to the fluid enhances the viscosity and density of the nanofluid.
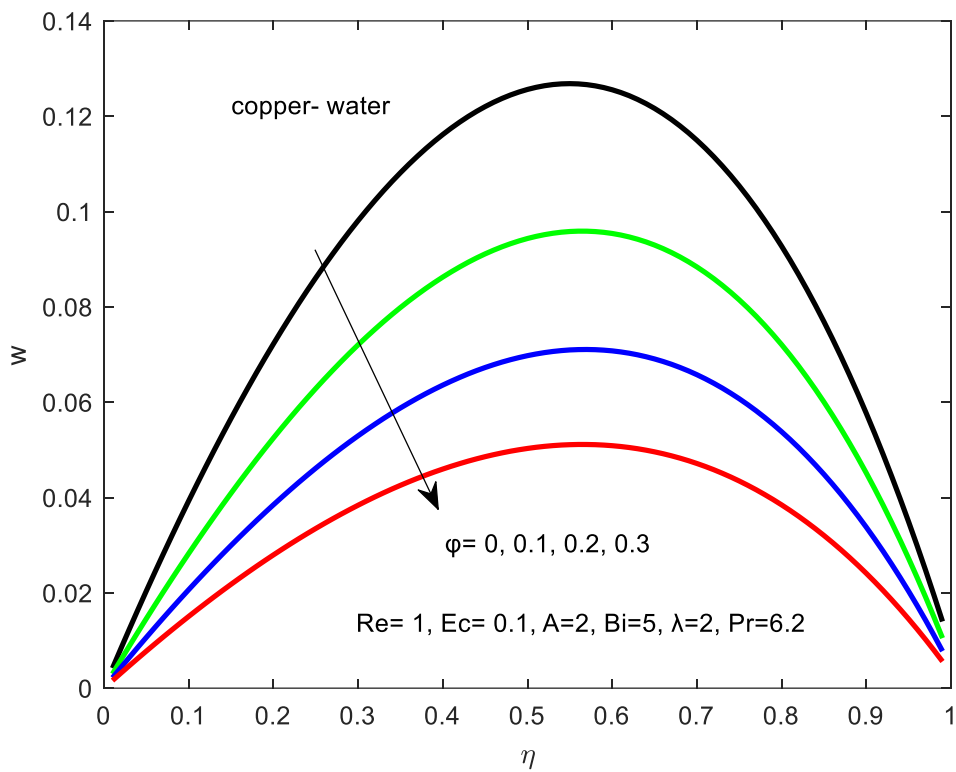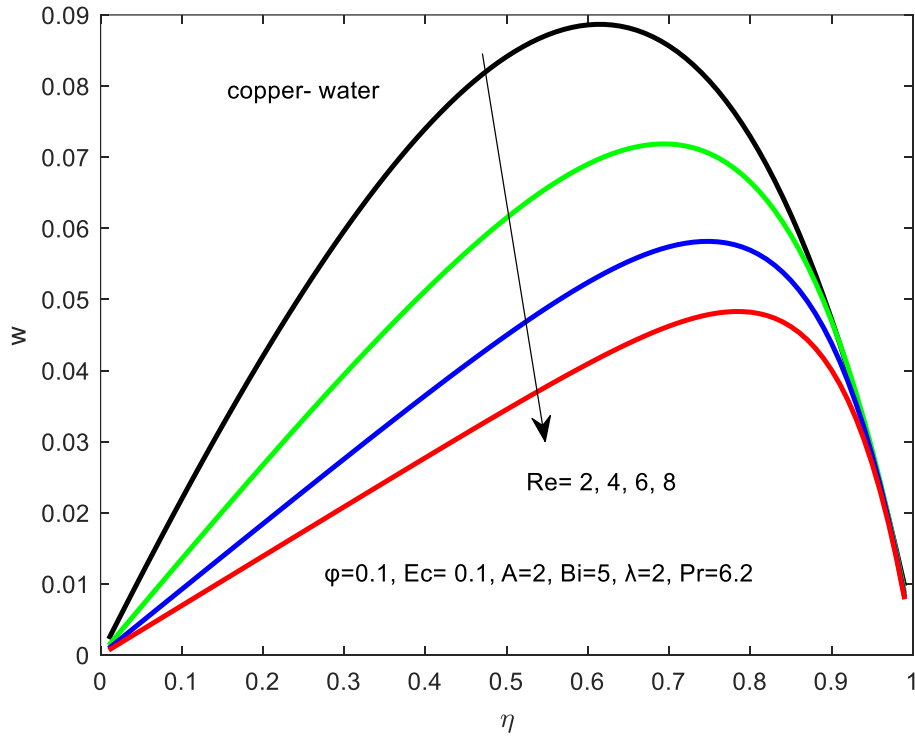
**Figure 10: Effect of velocity profiles with increase in φ**
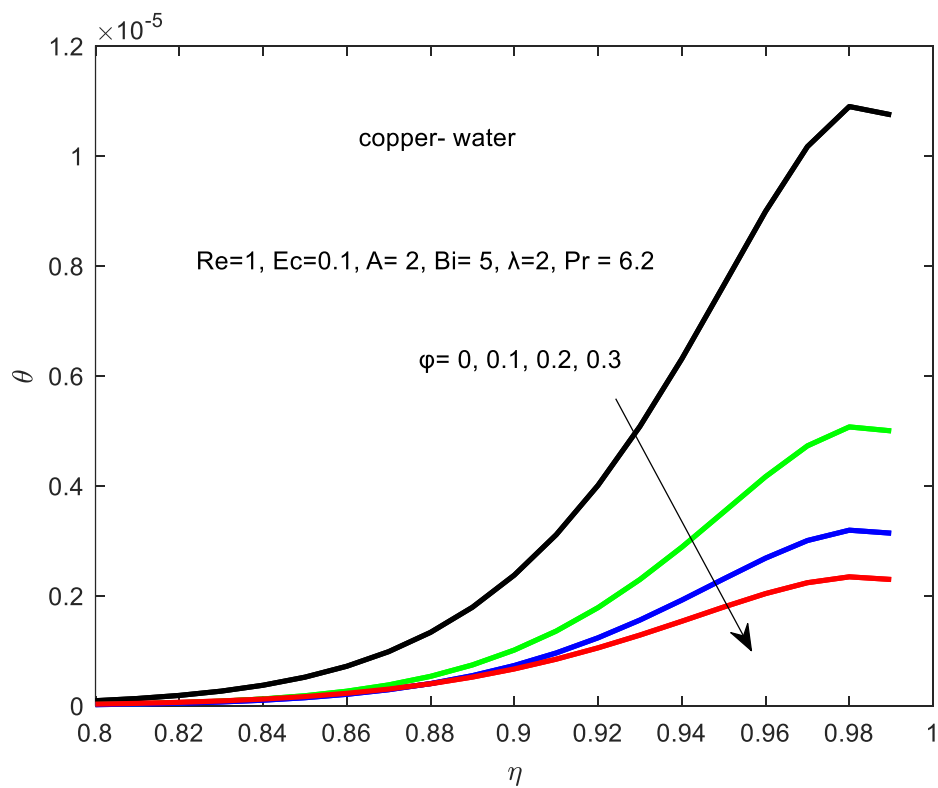
Figure 11: Effect of increase in φ on temperature profile

An increase in Reynold number causes a drop in velocity and temperature because the flow is smooth and orderly with high viscosity of nanofluid as revealed in Fig. 12 and Fig. 13, but the temperature begins to rise as it approaches the pipe's wall due to slip at the walls.
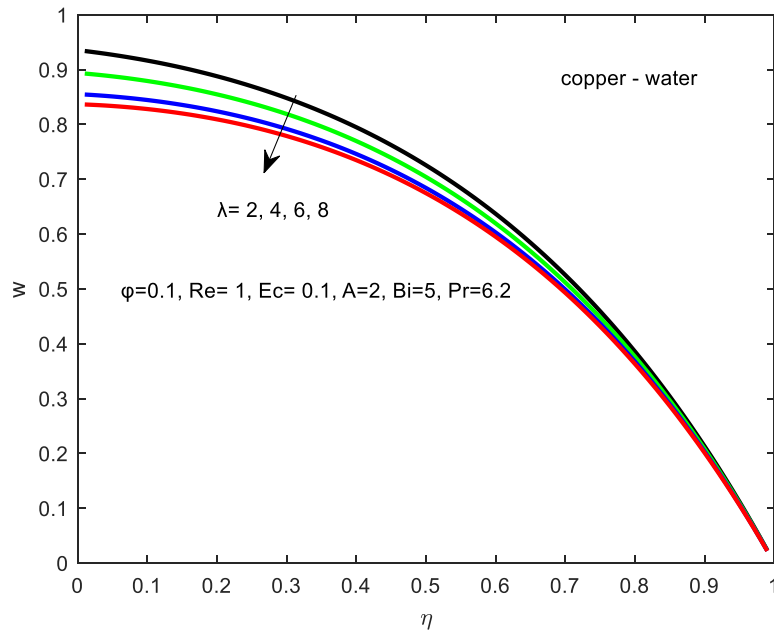

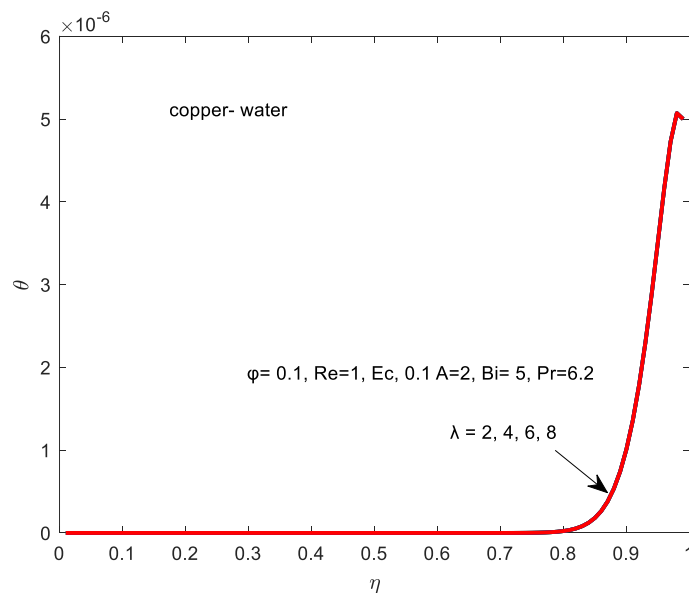**Figure 12: Effect of velocity profiles with increase in Re**
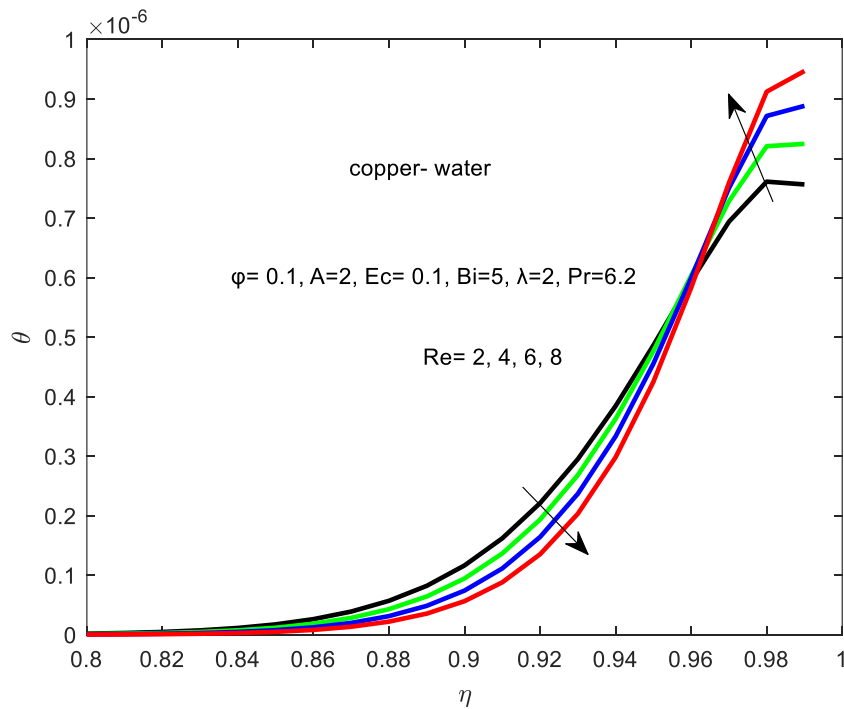
Figure 13: Effect of increase in Re on temperature profile

Figure 14 shows, the relationship of velocity and slip parameter (λ) they are inversely proportional since during the flow fluid sticks at the wall and cause the speed to be low. Moreover, because to the fluid's viscosity. Figure 15 shows that there is no effect of slip parameter increase on temperature profile.
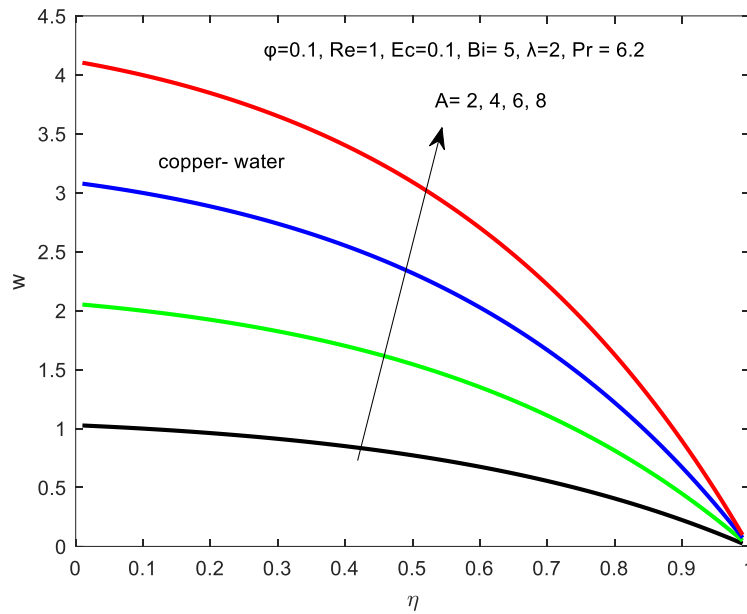

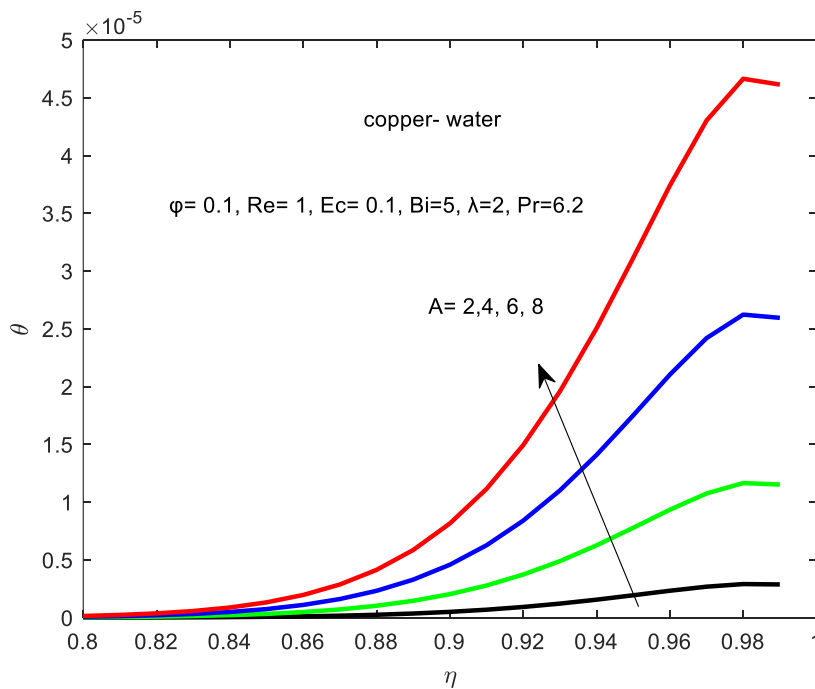Figure 14: Effect of velocity profiles with increase in λ

Figure 15: Effect of temperature profile with increase in λ

In Fig. 16 and Fig. 17 what is observed is that when pressure gradient (A) increase the velocity and temperature also increase due to the fact that the viscosity is reduced hence during the nanofluid flow the speed will increase and also since pressure gradient it depends on position

in other way we can say that is inversely proportional to distance these shows that by the start the pressure gradient was low when increase velocity starts also to increase.

Figure 16: Effect of velocity profiles with increase in A

Figure 17: Effect of temperature profile with increase in A

In Fig. 18 and Fig. 19, shows that increase of nanofluid velocity and temperature is detected with an increase in Eckert number (Ec) since the viscosity is reduced this implies that the speed or velocity during nanofluid flow is high and cause kinetic energy to be and figure high at the wall during the flow.

33

The relationship between an increase in Biot number (Bi) and a decrease in temperature is presented in Fig. 20, which indicates that heat is lost through the wall during the flow of the nanofluid.

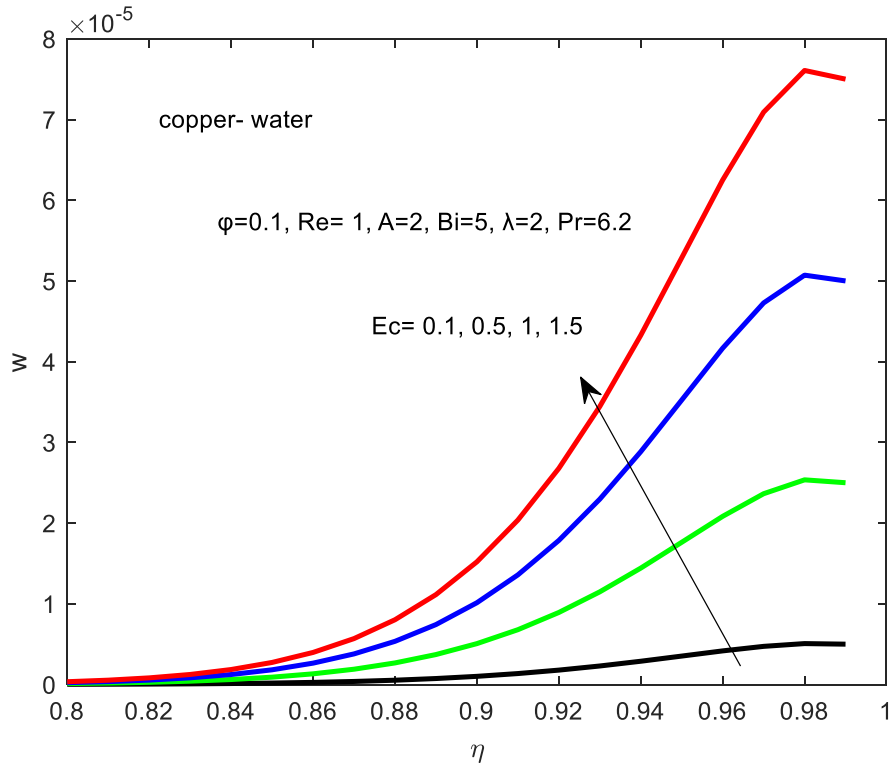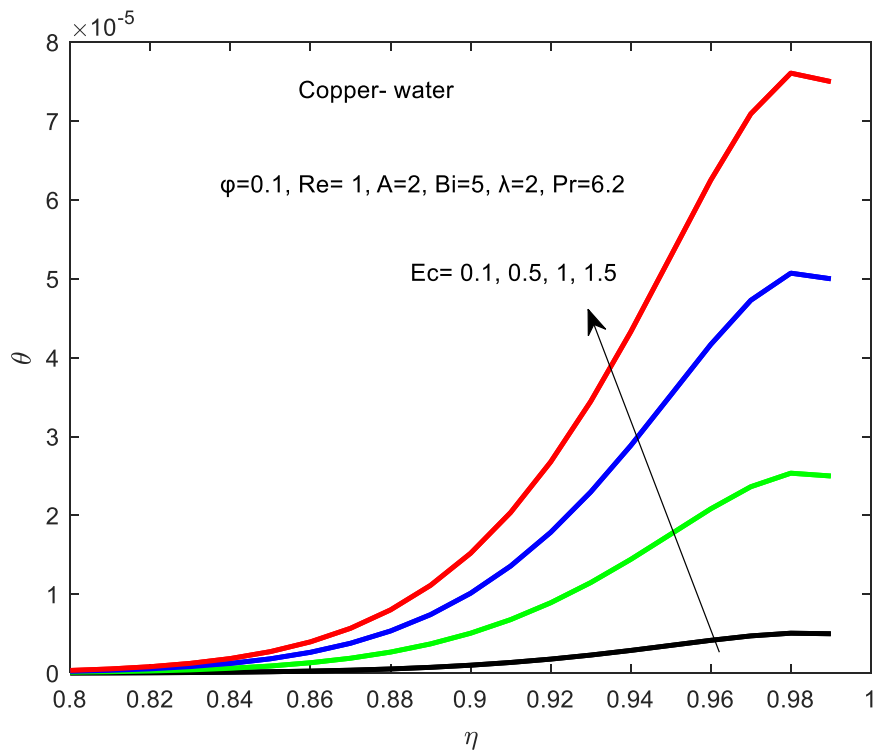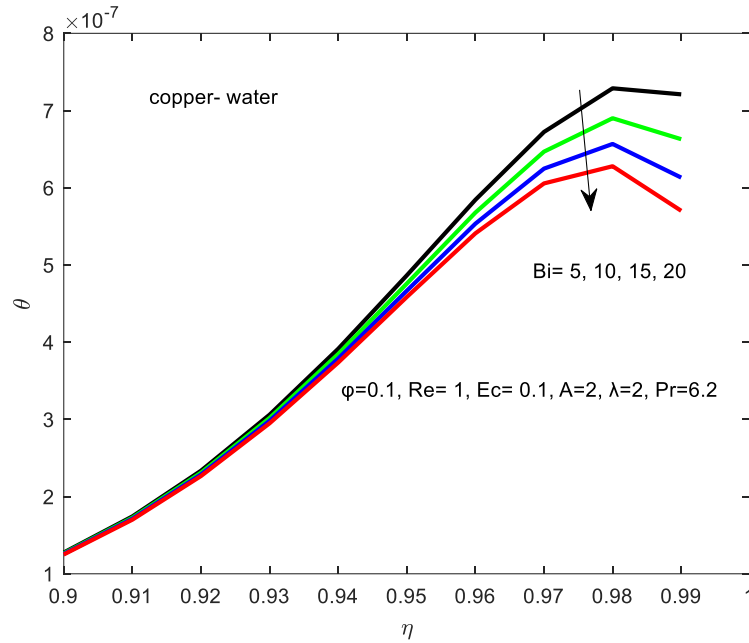**Figure 18: Effect of velocity profiles with increase in Ec**

Figure 19: Effect of temperature profile with increase in Ec

Figure 20: Effect of temperature profile with increase in Bi

4.2 Effect of parameter variation on Skin Friction and Nusselt Number

As demonstrated in Fig. 21, Alumina-water and Copper-water have different velocity gradients close to the channel walls. Due to that, skin friction of copper nanofluid is greater than of alumina. This discrepancy could be the result of Alumina's lower specific heat capacity than Copper.
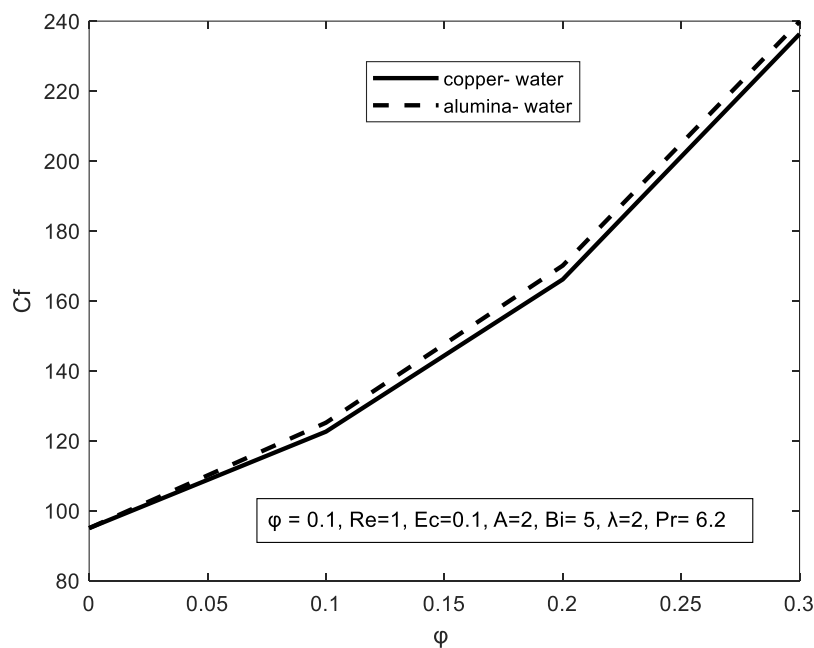
Figure 21: Effect of Skin friction on copper and alumina nanofluids

Figure 22 displays the effect of skin friction when we increase Navier slip. We have observed that the value of skin friction is high when we increase the Navier slip and it reaches some point we observe the slightly changes hence when the skin friction is high we need to add more value of nanoparticles.
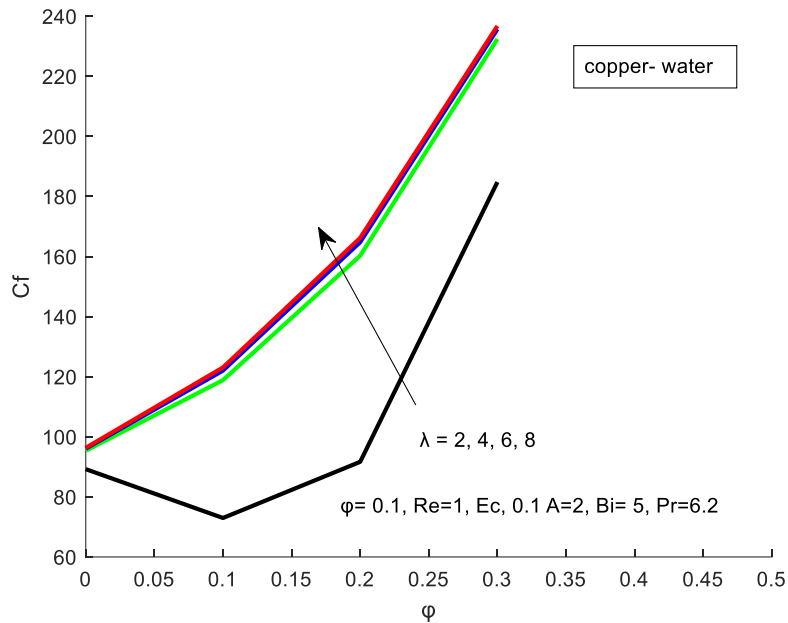

Figure 22: Effect of Skin friction with increase in λ

Figure 23, shows the results of skin friction and slip parameter. Since we have the slip parameter we expect the decrease of skin friction when we increase Reynold number. In Fig. 24, shows the effect of skin friction with the increase of pressure gradient. The Pressure gradient varies inversely proportional to the Skin friction decrease hence the flow velocity goes on decreasing as the kinetic energy of the layer is used to overcome the frictional resistance of the surface.
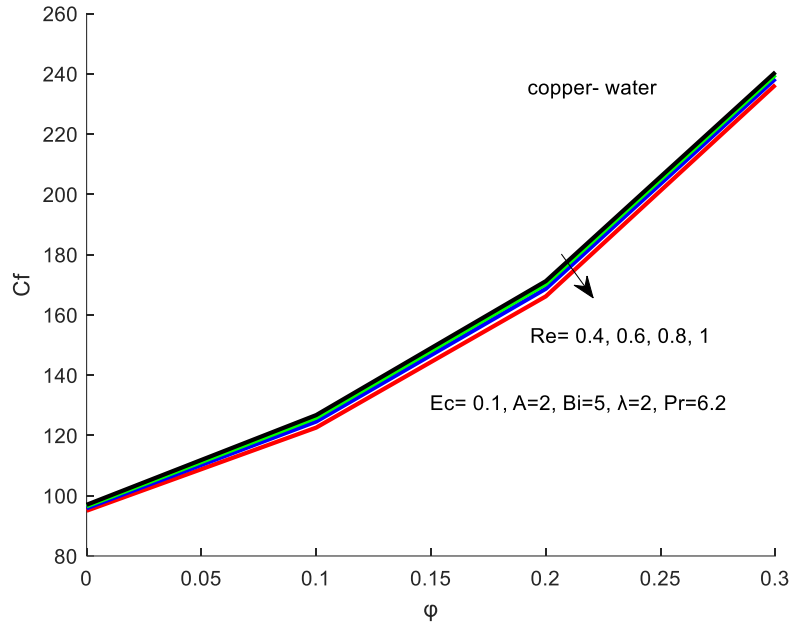
Figure 23: Effect of Skin friction with increase in Re
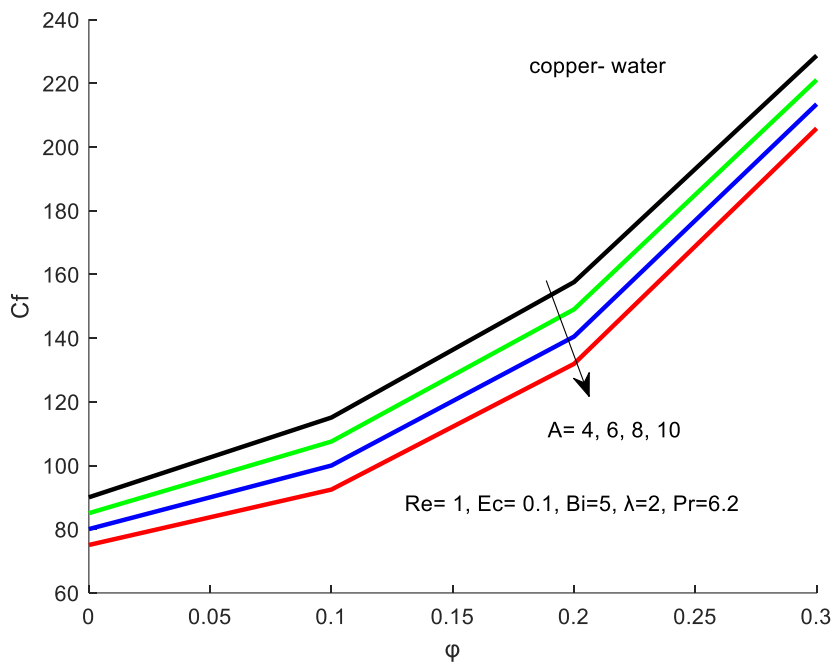
Figure 24: Effect of Skin friction with increase in A

In Fig. 25 and Fig. 26 shows the effect of increasing of Reynolds number and pressure gradient. Results are, the Reynolds number and the pressure gradient are directly proportional to Nusselt number due to the increase of speed which leads to produce more heat and lead to the reduction of viscosity.
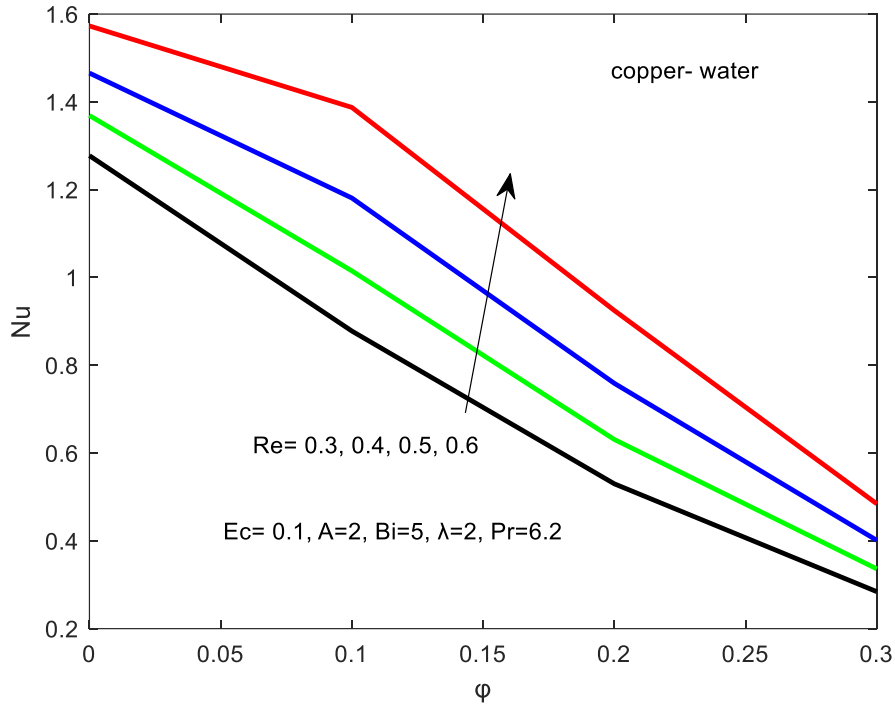
Figure 25: Effect of Nusselt number with increasing in Re
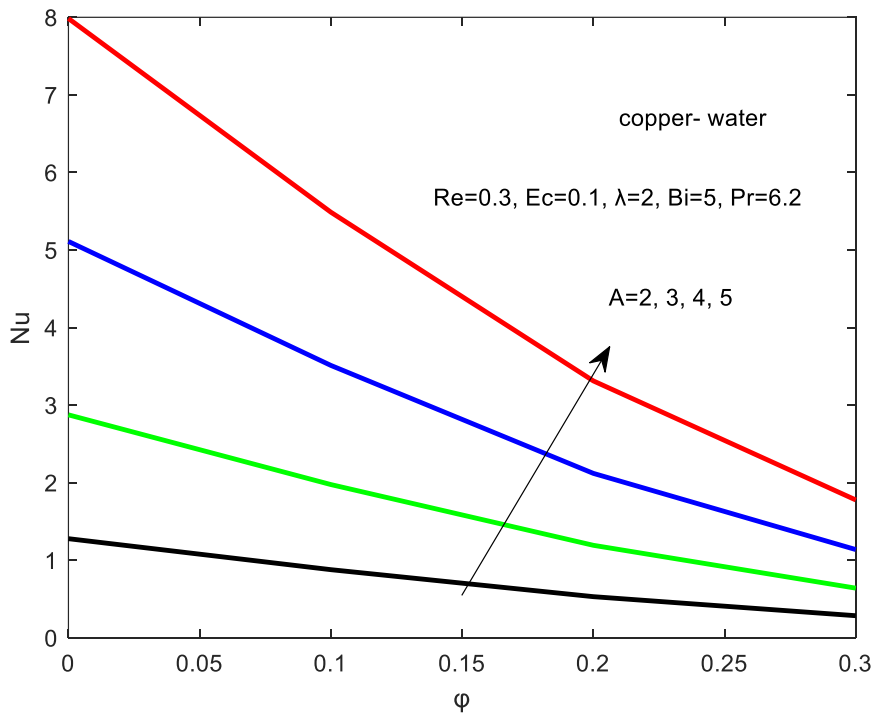
Figure 26: Effect of Nusselt number with increasing in A

Figure 27, Nusselt number also increases by means of the increase of Biot number may be this is because the fluid has a high thermal conductivity hence viscosity is reduced. The relationship of Nusselt number and slip parameter is presented in Fig. 28 are inversely proportional to each other due to convective cooling during the flow. In Fig. 29 Nusselt number increases with the

increase of Eckert number because during the flow when kinetic energy increase the temperature rise which cause more heat to be generated during the flow.

Figure 27: Effect of Nusselt number with increasing in Bi
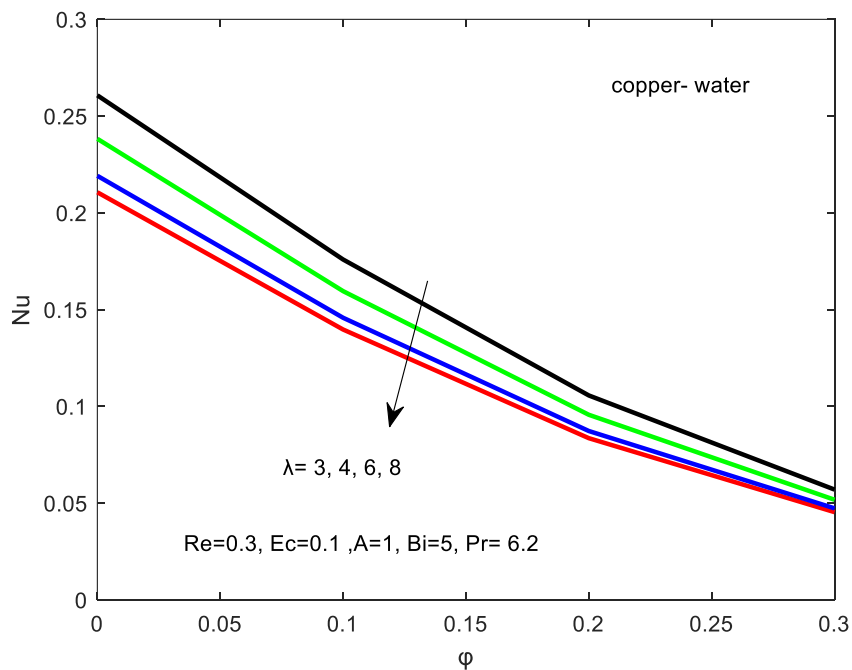
Figure 28: Effect of Nusselt number with increasing in λ
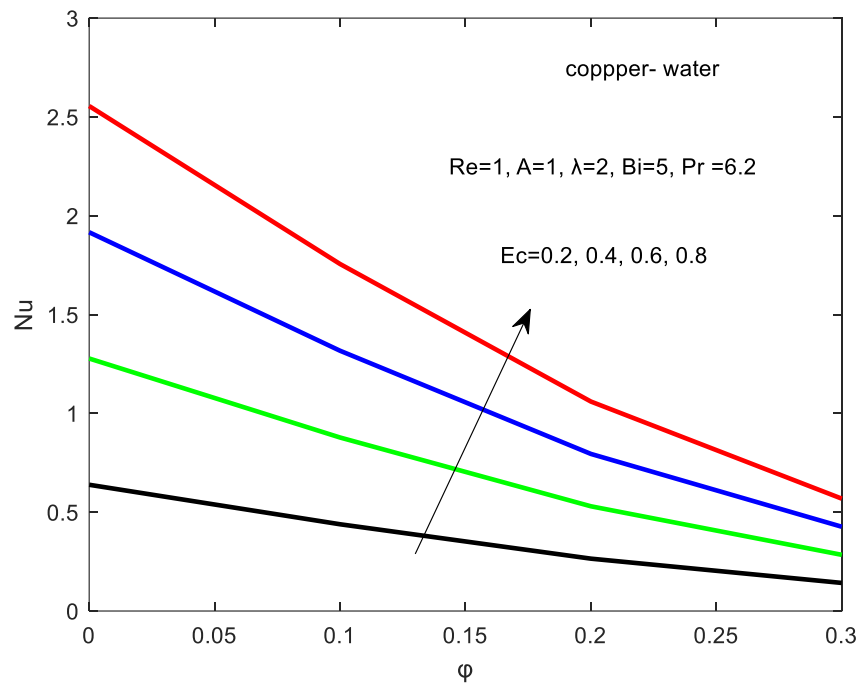
Figure 29: Effect of Nusselt number with increasing in Ec

CHAPTER FIVE

CONCLUSION AND RECOMMENDATIONS

5.1   Conclusion

This work has examined into the effects of skin friction and Navier slip on nanofluid flow in porous pipes. The line method is used to numerically solve the simplified system of differential equations. The observed conclusions are listed below:
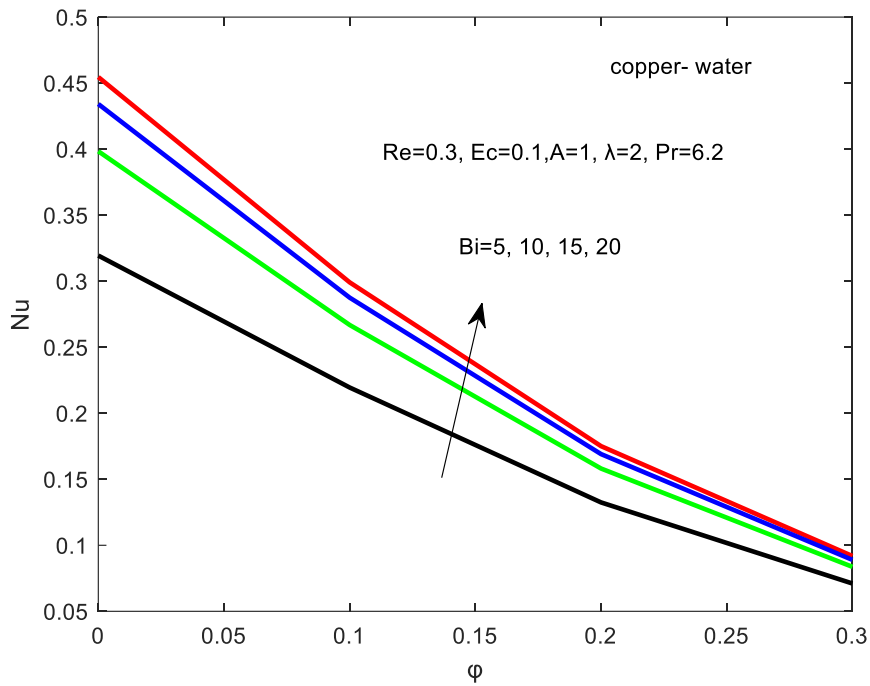
(i)   Reynolds number and Eckert number improve velocity and temperature. When the temperature drops with increase of Biot number and the Navier slip parameter causes a decrease in velocity.

(ii)   In comparison of alumina and copper-water nanofluid, the temperature and velocity of copper nanofluid rise more quickly than that of alumina.

(iii)   Pressure gradient is inversely proportional to skin friction, and when the skin friction is high to overcome that problem, it is important to add nanoparticle in the base fluid. Skin friction is retarded by increase Reynolds number. An increase of Reynolds number, Biot number and Eckert number causes an increase of heat transfer at the wall but for slip parameter is vice versa. Navier slip minimizes friction in the porous pipes close to the wall. Because of that the energy transfer coefficient is larger in a linear thermal distribution than a non-linear thermal distribution.

5.2   Recommendations

In order to overcome Skin friction during the flow there it is important to use nanofluid during the flow. Which will be useful to engineers in different application.

REFERENCES

Barik, R. N., Dash, G. C., & Rath, P. K. (2018). Steady laminar MHD flow of visco-elastic fluid through a porous pipe embedded in a porous medium. *Alexandria Engineering Journal*, *57*(2), 973-982. https://doi.org/10.1016/j.aej.2017.01.025

Bhatti, K., Bano, Z., & Siddiqui, A. M. (2018). Unsteady Stokes Flow through Porous Channel with Periodic Suction and Injection with Slip Conditions. *European Journal of Pure and Applied Mathematics*, *11*(4), 937–945. https://doi.org/10.29020/nybg.ejpam.v11i4.3309

Eegunjobi, A. S., & Makinde, O. D. (2012). Effects of navier slip on entropy generation in a porous channel with suction/injection. *Journal of Thermal Science and Technology*, *7*(4), 522–535. https://doi.org/10.1299/jtst.7.522

Eijkel, J. (2007). Liquid slip in micro-and nanofluidics: recent research and its possible implications. *Lab on a Chip*, *7*(3), 299-301. https://doi.org/10.1039/b700364c

Erdoğan, M. E., & İmrak, C. E. (2008). On the flow in a uniformly porous pipe. *International Journal of Non-Linear Mechanics*, *43*(4), 292-301.

Fang, M., Gilbert, R. P., & Liu, X. (2010). A squeeze flow problem with a Navier slip condition. *Mathematical and Computer Modelling*, *52*(1–2), 268–277. https://doi.org/10.1016/j.mcm.2010.02.024.

Mkwizu, M. H., Makinde, O. D., & Nkansah-Gyekye, Y. (2015). Effects of Navier slip and wall permeability on entropy generation in unsteady generalized Couette flow of nanofluids with convective cooling. *UPB Scientific Bulletin*, *77*(4), 201-216.

Flack, K. A., Schultz, M. P., Barros, J. M., & Kim, Y. C. (2016). Skin-friction behavior in the transitionally-rough regime. *International Journal of Heat and Fluid Flow*, *61*, 21–30. https://doi.org/10.1016/j.ijheatfluidflow.2016.05.008

Hussain, S., Aziz, A., Aziz, T., & Khalique, C. M. (2016). Slip flow and heat transfer of nanofluids over a porous plate embedded in a porous medium with temperature dependent viscosity and thermal conductivity. *Applied Sciences*, *6*(12), 1-17. https://doi.org/10.3390/app6120376

Kalyon, D. M. (2005). Apparent slip and viscoplasticity of concentrated suspensions. *Journal of Rheology*, *49*(3), 621–640. https://doi.org/10.1122/1.1879043

Kasaeian, A., Azarian, R. D., Mahian, O., Kolsi, L., Chamkha, A. J., Wongwises, S., & Pop, I. (2017). Nanofluid flow and heat transfer in porous media: A review of the latest developments. *International Journal of Heat and Mass Transfer*, *107*, 778–791. https://doi.org/10.1016/j.ijheatmasstransfer.2016.11.074

Khamis, S., Makinde, O. D., & Nkansah-Gyekye, Y. (2015). Buoyancy-driven heat transfer of water− based nanofluid in a permeable cylindrical pipe with navier slip through a saturated porous medium. *Journal of Porous Media, 18*(12), 1169-1180

Gadanga, A. T., & Chukwuji, C. N. (2020). International Journal of Science for Global Sustainability (IJSGS): A Bibliometric Analysis: 2015-2019. *International Journal of Science for Global Sustainability*, *6*(1), 13-13.

Mahmoudi, Y., & Karimi, N. (2014). International Journal of Heat and Mass Transfer Numerical investigation of heat transfer enhancement in a pipe partially filled with a porous material under local thermal non-equilibrium condition. *International Journal of Heat and Mass Transfer*, *68*, 161–173. https://doi.org/10.1016/j.ijheatmasstransfer.2013.09.020

Makinde, O. D., Khamis, S., Tshehla, M. S., & Franks, O. (2014). Analysis of heat transfer in Berman flow of nanofluids with navier slip, viscous dissipation, and convective cooling. *Advances in Mathematical Physics*, *2014*, 1-14. https://doi.org/10.1155/2014/809367

Mari, J. L. (1987). Modelling of the skin friction and heat transfer in turbulent two-component bubbly flows in pipes. *International Journal of Multiphase Flow*, *13*(3), 309-325.

Morton, K. W., & Mayers, D. F. (2005). *Numerical solution of partial differential equations: An introduction*. Cambridge University Press. https://assets.cambridge.org/97805216/07933/frontmatter/9780521607933_frontmatter.pdf

Muravleva, L. (2017). Axisymmetric squeeze flow of a viscoplastic Bingham medium. *Journal of Non-Newtonian Fluid Mechanics*, *249*, 97–120. https://doi.org/10.1016/j.jnnfm.2017.09.006

Mutuku-Njane, W. N., & Makinde, O. D. (2013). Combined effect of Buoyancy force and Navier slip on MHD flow of a nanofluid over a convectively heated vertical porous plate. *The Scientific World Journal*, *2013*, 1-9. https://doi.org/10.1155/2013/725643

Nair, K. A., & Sameen, A. (2015). Experimental study of slip flow at the fluid-porous interface in a boundary layer flow. *Procedia IUTAM*, *15*, 293-299. https://doi.org/10.1016/j.piutam.2015.04.041.

Nouri-Borujerdi, A., & Seyyed-Hashemi, M. H. (2015). Numerical analysis of thermally developing turbulent flow in partially lled porous pipes. *Scientia Iranica*, *22*(3), 835-843.

Pandey, A. K., & Kumar, M. (2017). Natural convection and thermal radiation influence on nanofluid flow over a stretching cylinder in a porous medium with viscous dissipation. *Alexandria Engineering Journal*, *56*(1), 55-62.

Rawi, N. A., Mohd Kasim, A. R., Isa, Z. M., Mangi, A., & Shafie, S. (2017). G-jitter effects on the mixed convection flow of nanofluid past an inclined stretching sheet. *Frontiers in Heat and Mass Transfer*, *2017,* 8-12. https://doi.org/10.5098/hmt.8.12

Rundora, L., & Makinde, O. D. (2014). *Effects of Navier slip and suction / injection on an unsteady reactive variable viscosity non-Newtonian fluid flow in a channel filled with porous medium and convective boundary conditions*. https://doi.org/10.2495/AFM140251

Sochi, T. (2011). Slip at fluid-solid interface. *Polymer Reviews*, *51*(4), 309-340.

Srinivas, S., Reddy, A. S., & Ramamohan, T. R. (2015). Mass transfer effects on viscous flow in an expanding or contracting porous pipe with chemical reaction. *Heat Transfer—Asian Research*, *44*(6), 552-567.

Srinivas, S., Vijayalakshmi, A., Reddy, A. S., & Ramamohan, T. R. (2016). MHD fl ow of a nano fl uid in an expanding or contracting porous pipe with chemical reaction and heat source / sink. *Propulsion and Power Research*, *5*(2), 134–148. https://doi.org/10. 1016/j.jppr.2016.04.004

Wang, C. Y., & Ng, C. (2011). International Journal of Non-Linear Mechanics Slip flow due to a stretching cylinder. *International Journal of Non-Linear Mechanics*, *46*(9), 1191–1194. https://doi.org/10.1016/j.ijnonlinmec.2011.05.014.

APPENDIX

```
function ds =
ode_sys3(t,s,delta_eta,Pr,Ec,Re,A,t1,ro1,ro2,phi,K1,K2,Bi
,n,m,lambda)
%input t the time variable (not used in this case)
% s the state vector
% k1,k2 model parameters
%output ds the derivative ds/dt at time t
for k=1:n
w(k) = s(k); %for clarity & readability, write th
theta(k) = s(n+k); %model using the notation A,B,C for the
%components
end
for k=1:n
    if(k==1)
        W1=0;
       THETA1=0;
        THETA2=theta(k+1);
          W2=w(k+1);
    elseif(k==n)
         W2=lambda*w(2)/(lambda-delta_eta);
    THETA2=THETA1-(2*Bi*theta(k)*delta_eta);
     THETA1=theta(k-1);
      W1=w(k-1);
    else
        W1=w(k-1);
    W2=w(k+1);
    THETA1=theta(k-1);
    THETA2=theta(k+1);
    end

dw(k)        =        A*(1-phi+phi*ro1*ro2^(-1))^(-1)+(((1-
phi)+phi*ro1*ro2^(-1))*(1-phi)^2.5)^(-1)*(W2-
2*w(k)+W1)*(delta_eta)^(-2)-Re*(W2-W1)*(2*delta_eta)^(-
1);
dtheta(k)             =(m*Pr*(1-phi+phi*t1))^(-1)*(THETA2-
2*theta(k)+THETA1)/(delta_eta)^2+Ec*((1-phi+phi*t1)*(1-
phi)^(2.5))^(-1)*((W2-W1)*(2*delta_eta)^(-1))^2-
Re*(THETA2-THETA1)*((2*(delta_eta))^(-1));
end

%%%%%%%%%%%%%%%%%%%%%%%%%%%%%%%%%%%%%%%%%%%%%%%%%%%%%%%%%%%%%
%%%%
%% SECTION TITLE
% DESCRIPTIVE TEXT
```

45

```matlab
% %close all
close all
clear all
clc
% c=['k','g','b','r'];
tspan = 0:0.01:10; %time interval with observations at
every integer
delta_eta=0.01;
n=1/delta_eta-1;
eta=delta_eta:delta_eta:1-delta_eta;
%eta=0:delta_eta:1;
s0 = [zeros(1,n),zeros(1,n)]; %initial values for x,y,z,m
Pr = 6.2; %model parameter 0.4

phi=0.1; %model parameter 0.01
lambda=2;

Re=1;
Ec=0.1; %model parameter 0.1
A=2;
Bi=5;%Biot number

ro2=997.1;%density of water
K2=0.613;%thermal condactivity of water
cp2=4176; %specifis heat of water

Br=Pr*Ec;

myname = {'Alumina-Water','Copper-water'};
K1 = [40 401]; cp1 = [765 385]; ro1 = [3970 8933];
ax = axes;
ax.ColorOrder = [0 0 0; 0 1 0; 0 0 1; 1 0 0];
ax.LineStyleOrder = {'-','--'};
% col = ['k','g','b','r'];
% cool =
for jj =1:length(K1)
    t1=(ro1(jj)*cp1(jj))*(ro2*cp2)^(-1);

    m=((K1(jj)+2*K2)+phi*(K2-K1(jj)))*...
        ((K1(jj)+2*K2)-2*phi*(K2-K1(jj)))^(-1);

    [t,s]                                        =
ode15s(@ode_sys3,tspan,s0,[],delta_eta,Pr,Ec,Re,A,t1,ro1(
jj),ro2,phi,K1(jj),K2,Bi,n,m,lambda);
    w1=s(:,1:n);
    theta1=s(:,n+1:2*n);
```

```matlab
hold on
txt = myname;
plot(t,theta1(:,0.6*(n+1)),'DisplayName',txt{jj},'LineWid
th',2)
hleg = legend('show');
plot(t,theta1(:,0.7*(n+1)),'LineWidth',2)
hleg.String(end) = [];
plot(t,theta1(:,0.8*(n+1)),'LineWidth',2)
hleg.String(end) = [];
plot(t,theta1(:,0.9*(n+1)),'LineWidth',2)
hleg.String(end) = [];

end
hold off
legend('Location','northwest')
legend show
  ylabel('w')
 xlabel('t')
box on


%%%%%%%%%%%%%%%%%%%%%%%%%%%%%%%%%%%%%%%%%%%%%%%%%%%%%%%%%%%%%%%
%% SECTION TITLE
% DESCRIPTIVE TEXT
% %close all
clear all
clc
 c=['k','g','b','r'];
tspan = 0:0.01:10; %time interval with observations at
every integer
 delta_eta=0.01;
 n=1/delta_eta-1;
 eta=delta_eta:delta_eta:1-delta_eta;
 %eta=0:delta_eta:1;
 s0 = [zeros(1,n),zeros(1,n)]; %initial values for x,y,z,m
Pr = 6.2; %model parameter 0.4
phi=0.1;

lambda=2;
Re=1;
var1=[0.1 0.5 1 1.5];
for j=1:4
   Ec=var1(j);
Bi=5; %model parameter 0.01;
```

47

```matlab
%Ec= 0.1; %model parameter 0.1
A=2;



ro2=997.1;%density of water
K2=0.613;%thermal condactivity of water
cp2=4176; %specifis heat of water



  Br=Pr*Ec;

 K1=401;%thermal condactivity of solid
  ro1=8933;%density of solid cu
  cp1=385;%specific of cu
  t1=(ro1*cp1)*(ro2*cp2)^(-1);
  m=((K1+2*K2)+phi*(K2-K1))*((K1+2*K2)-2*phi*(K2-K1))^(-
1);

[t,s]                                            =
ode15s(@ode_sys3,tspan,s0,[],delta_eta,Pr,Ec,Re,A,t1,ro1,
ro2,phi,K1,K2,Bi,n,m,lambda);
 w1=s(:,1:n);
 theta1=s(:,n+1:2*n);



%plot(eta,w1(100,:),c(:,j),'LineWidth',2)
  plot(eta,theta1(2,:),c(:,j),'LineWidth',2)
      hold on
    end
% % % % % %  ylim([0 4])
% % % % % %  xlim([0 1])
% % % % % %  %title('Solution Curves for the Model')
 %ylabel('\theta')
ylabel('w')
xlabel('\eta')
 xlim([0.8 1])
%  %legend ('Alumina','Cupper','Water only')



%%%%%%%%%%%%%%%%%%%%%%%%%%%%%%%%%%%%%%%%%%%%%%%%%%%%

%% SECTION TITLE
% DESCRIPTIVE TEXT
% %close all
clear all
clc
```

```
 c=['k','g','b','r'];
tspan = 0:0.01:10; %time interval with observations at
every integer
 delta_eta=0.01;
 n=1/delta_eta-1;
 eta=delta_eta:delta_eta:1-delta_eta;
 %eta=0:delta_eta:1;
 s0 = [zeros(1,n),zeros(1,n)]; %initial values for x,y,z,m
Pr = 6.2; %model parameter 0.4
%a=1;
%c=['k','r','b'];
A=2; %model parameter 0.01
lambda=2;
var1=[0 0.1 0.2 0.3];
for i=1:4
    phi=var1(i);
Re=1;
Ec=0.5; %model parameter 0.1
%phi=0.1;
Bi=5;%Biot number

ro2=997.1;%density of water
K2=0.613;%thermal condactivity of water
cp2=4176; %specifis heat of water


   Br=Pr*Ec;

%   ro1=3970; %alu
%   K1=40;%alu
%   cp1=765;%specific of alu
%   t1=(ro1*cp1)*(ro2*cp2)^(-1);
%   m=((K1+2*K2)+phi*(K2-K1))*((K1+2*K2)-2*phi*(K2-K1))^(-
1);

  ro1=8933;%density of solid cu
  K1=401;%thermal condactivity of solid
  cp1=385;%specific of cu
  t1=(ro1*cp1)*(ro2*cp2)^(-1);
  m=((K1+2*K2)+phi*(K2-K1))*((K1+2*K2)-2*phi*(K2-K1))^(-
1);

[t,s]                                        =
ode15s(@ode_sys3,tspan,s0,[],delta_eta,Pr,Ec,Re,A,t1,ro1,
ro2,phi,K1,K2,Bi,n,m,lambda);
 w1=s(:,1:n);
 theta1=s(:,n+1:2*n);
```

```matlab
% %

 %SKIN AND NUSL
%                 nu(i)=-1/m*((theta1(end,end)/(delta_eta*(1-
m*Bi*delta_eta)))-theta1(end,end)/delta_eta);
 %nu(i)=Bi*theta1(end,end);
sk(i)=((1-phi)^(-2.5))*(1-w1(end,end))*(delta_eta)^(-1);
end
  ylabel('Cf')
  xlabel('?')


%%%%%%%%%%%%%%%%%%%%%%%%%%%%%%%%%%%%%%%%%%%%%%%%%%%%%%%%%%
%% SECTION TITLE
% DESCRIPTIVE TEXT
% %close all
%clear all
clc
 c=['k','g','b','r'];
tspan = 0:0.01:10; %time interval with observations at
every integer
 delta_eta=0.01;
 n=1/delta_eta-1;
 eta=delta_eta:delta_eta:1-delta_eta;
 %eta=0:delta_eta:1;
 s0 = [zeros(1,n),zeros(1,n)]; %initial values for x,y,z,m
Pr = 6.2; %model parameter 0.4
%a=1;
%c=['k','r','b'] ;
A=2; %model parameter 0.01
lambda=2;

Re=1;
Ec=0.1; %model parameter 0.1
phi=0.1;
Bi=5;%Biot number
%the pressure gradient parameter
%d=2;
ro2=997.1;%density of water
K2=0.613;%thermal condactivity of water
cp2=4176; %specifis heat of water


   Br=Pr*Ec;
%   ro1=3970; %alu
%   K1=40;%alu
%   cp1=765;%specific of alu
```

50

```matlab
%    t1=(ro1*cp1)*(ro2*cp2)^(-1);
%    m=((K1+2*K2)+phi*(K2-K1))*((K1+2*K2)-2*phi*(K2-K1))^(-1);

  ro1=8933;%density of solid cu
  K1=401;%thermal condactivity of solid
  cp1=385;%specific of cu
  t1=(ro1*cp1)*(ro2*cp2)^(-1);
  m=((K1+2*K2)+phi*(K2-K1))*((K1+2*K2)-2*phi*(K2-K1))^(-1);

[t,s]                                                  =
ode15s(@ode_sys3,tspan,s0,[],delta_eta,Pr,Ec,Re,A,t1,ro1,
ro2,phi,K1,K2,Bi,n,m,lambda);
 w1=s(:,1:n);
 theta1=s(:,n+1:2*n);

  figure
%
%
%%%%%%%%%%%%%%%%%%%%%%%%%%%%%%%%%%%%%%%%%%%%%%%%%%%%%%%%%%%%%%
%%%%%
plot(t,w1(:,0.5*(n+1)),'k','LineWidth',2)
hold on
plot(t,w1(:,0.6*(n+1)),'g','LineWidth',2)
plot(t,w1(:,0.7*(n+1)),'b','LineWidth',2)
plot(t,w1(:,0.8*(n+1)),'r','LineWidth',2)
 %title('Solution Curves for the Model')
 ylabel('w')
 xlabel('t')
%    xlim([0 1])
 figure
plot(t,theta1(:,0.6*(n+1)),'k','LineWidth',2)
 hold on
plot(t,theta1(:,0.7*(n+1)),'g','LineWidth',2)
plot(t,theta1(:,0.8*(n+1)),'b','LineWidth',2)
plot(t,theta1(:,0.9*(n+1)),'r','LineWidth',2)
% title('Solution Curves for the Model')
 ylabel('\theta')
 xlabel('t')
 %ylim([0 0.1])
% xlim([0 4])

%
%%%%%%%%%%%%%%%%%%%%%%%%%%%%%%%%%%%%%%%%%%%%%%%%%%%%%%%%%%%%%%
%%%%%%%%%%%
figure
```

```matlab
plot(eta,w1(10,:),'k','LineWidth',2)
hold on
plot(eta,w1(30,:),'g','LineWidth',2)
plot(eta,w1(50,:),'b','LineWidth',2)
plot(eta,w1(100,:),'r','LineWidth',2)
 %title('Solution Curves for the Model')
 ylabel('w')
 xlabel('\eta')
% ylim([0 1.2])
%  %xlim([0 2])
  figure
plot(eta,theta1(10,:),'k','LineWidth',2)
hold on
plot(eta,theta1(20,:),'g','LineWidth',2)
plot(eta,theta1(40,:),'b','LineWidth',2)
plot(eta,theta1(50,:),'r','LineWidth',2)
%  %title('Solution Curves for the Model')
 ylabel('\theta')
 xlabel('\eta')
% %  xlim([0 0.8])
```

RESEARCH OUTPUTS

(i)   Publication Paper

Muyungi, W. N., Mkwizu, M. H., & Masanja, V. G. (2022). The Effect of Navier Slip and Skin Friction on Nanofluid Flow in a Porous Pipe. *Engineering, Technology and Applied Science Research*, *12*(2), 8342-8348.

(ii)   Poster Presentation

Effects of Navier Slip and Skin Friction on Nanofluid Flow in a Porous Pipe